

Streamflow drought: implication of drought definitions and its application for drought forecasting

Samuel J. Sutanto¹ and Henny A. J. Van Lanen¹

¹Hydrology and Quantitative Water Management Group, Environmental Sciences Department, Wageningen University and Research, Droevendaalsesteeg 3a, 6708PB, Wageningen, the Netherlands

Correspondence: Samuel Sutanto (samuel.sutanto@wur.nl)

Abstract. Streamflow drought forecasting is a key element of contemporary Drought Early Warning Systems (DEWS). The term streamflow drought forecasting (not streamflow forecasting), however, has created confusion within the scientific hydro-meteorological community, as well as in operational weather and water management services. Streamflow drought forecasting requires an additional step, which is the application of a drought identification method to the forecasted streamflow time series. The way, how streamflow drought is identified, is the main reason for this misperception. The purpose of this study, therefore, is to provide a comprehensive overview of the differences of streamflow droughts using different identification approaches for European rivers, including an analysis of both historical drought and implications for forecasting. Streamflow data were obtained from the LISFLOOD hydrological model forced with gridded meteorological observations (known as LISFLOOD-Simulation Forced with Observed, SFO). The same model fed with seasonal meteorological forecasts of the European Centre for Medium-range Weather Forecasts system 5 (ECMWF SEAS 5) was used to obtain the forecasted streamflow. Streamflow droughts were analyzed using the daily and monthly Variable Threshold methods (VTD and VTM), daily and monthly Fixed Threshold methods (FTD and FTM), and the Standardized Streamflow Index (SSI). Our results clearly show that streamflow droughts derived from different approaches deviate from each other in their characteristics, which also vary in different climate regions across Europe. The daily threshold methods (FTD and VTD) identify 25-50% more drought events as the monthly threshold methods (FTM and VTM) and accordingly the average drought duration is longer for the monthly than for the daily threshold method. The fixed threshold methods (FTs, FTD, and FTM), in general, identify earlier drought than the variable threshold methods (VTs, VTD, and VTM). In addition, the droughts obtained with monthly identification approaches also have higher drought deficit volumes (about 25-30%) than the daily approaches. Overall, the characteristics of SSI-1 drought are more or less similar to what is being identified by the monthly threshold approaches (FTM and VTM). The different outcome obtained with the drought identification methods illustrated with the historical analysis is also found in drought forecasting, as documented for the 2003 drought across Europe and for the Rhine River specifically. To the end, there is no unique hydrological drought definition (identification method) that fits all purposes, hence developers of DEWS and end-users should clearly agree in the co-design phase upon a sharp definition on which type of streamflow drought is required to be forecasted for a specific application.

1 Introduction

Drought is a creeping natural disaster that has major socio-economic and environmental impacts across the world (e.g., Tallaksen and Van Lanen , 2004; Wilhite et al. , 2007; Ding et al., 2011; Van Dijk et al. , 2013; Stahl et al., 2016; Haile et al. , 2019). The IPCC (2014) reports with very high confidence that impacts from among others drought on society are already
30 considerable. Drought hazard and their impacts are projected to increase in numerous regions under a future warmer climate (e.g., Feyen and Dankers , 2009; Forzieri et al., 2014; Prudhomme et al., 2014; Wanders et al. , 2015; Samaniego et al., 2018). Gu et al. (2020) analyzed how drought influences regional gross domestic product (GDP) under different representative concentration pathways (RCPs) and shared socioeconomic pathways (SSPs) at the global scale. The fraction of drought-affected GDP relative to the country's GDP would equal 100% in over about 75 countries under 1.5°C warming, which is projected
35 to increase to over 90 countries under 2.0°C warming. There is an urgent necessity for society to respond to these signs. National Drought Policy Plans (NDPPs) should be implemented that convert the usually reactive drought crisis management into a pro-active risk management (Sivakumar et al., 2014; WMO and GWP , 2014; Poljanšek et al., 2017). One of the elements to be included in the NDPP is a Drought Early Warning System (DEWS) that in addition to real-time monitoring contains operational drought forecasting with appropriate lead times (i.e. multi-months or seasonal).

40 The term drought forecasting has been used in an indefinite way, which has created misconceptions, miss-citations, and confusion in the scientific hydro-meteorological community (authors, readers, editors, and reviewers), as well as among policy makers, and in operational weather and water management services. An explicit definition of what is being forecasted is crucial to avoid any misunderstanding on the usability of drought forecast products for different purposes. Firstly, meteorological drought forecast systems have been developed (e.g., Mishra and Desai , 2005; Belayneh et al., 2014; Dutra et al., 2014), which
45 frequently use the Standardized Precipitation Index, SPI (McKee et al., 1993), or the Standardized Precipitation Evaporation Index, SPEI (Vicente-Serrano et al., 2010). These aggregate precipitation (SPI), and precipitation minus potential evaporation (SPEI) over at least one month and have lead times of one to several months. It should be noted that conventional weather forecast systems, which predict low or no precipitation and above normal temperature, as part of their regular suite of forecast products, should be not classified as a drought forecasting system, because of their rather short lead time (sub-daily to 10-15
50 days). Secondly, hydrological drought forecasts are provided (e.g., Pozzi et al., 2013; Sutanto et al., 2020a), which involve groundwater, river flow, soil moisture, and runoff. Hydrological drought deviates from meteorological drought (e.g., Changnon , 1987; Peters et al., 2003; Mishra and Singh, 2010; van Loon and van Lanen , 2012; Barker et al., 2016; Sutanto et al., 2020b), which means that the latter cannot straightforwardly be used to predict drought in groundwater or river flow. Because of all these differences, an explicit delineation of what is being forecasted is a prerequisite. Here, our study focuses on streamflow
55 drought forecasting, as part of hydrological drought forecasting, which is defined as below-normal streamflow (Hisdal et al. , 2004; Peters et al., 2006; Fleig et al., 2006; Feyen and Dankers , 2009; Sarailidis et al., 2019).

Forecasting of streamflow drought follows different approaches on how the hydrological drought is defined (Hisdal et al., 2004; van Loon, 2015), which is also essential to consider when using forecast products. Yuan et al. (2017) use the so-called standardized approach. They forecasted the Standardized Streamflow Index (SSI), which measures monthly normalized anomalies in streamflow and, if negative, then SSI signifies a dry anomaly. Others applied the threshold approach to predict drought in river flow from the forecasted flow time series. This implies that the river is in drought when it is below a predefined flow. Marx et al. (2018) and Wanders et al. (2019) use a fixed threshold meaning that it does not vary throughout the year. Usually, a percentile of the flow duration curve is taken using all flow data to identify the fixed threshold. On the contrary, Fundel et al. (2013), Sutanto et al. (2020a), and van Hateren et al. (2019) have used the variable threshold approach to identify drought events with their hydrological drought forecasting system. In this approach, the threshold varies over the year and accounts for seasonality, which means that forecasted drought can occur in every season. The threshold is derived from, for instance, the daily, monthly, or seasonal flow duration curve.

In the context of this study, it is also important to note, that hydrological drought forecasting is different from just streamflow forecasting (e.g., Day, 1985; Clark and Hay, 2004; Schaake et al., 2007; Bell et al., 2017; Mendoza et al., 2017; Arnal et al., 2018; Duan et al., 2019), although the latter provides key input data to derive hydrological drought. For hydrological drought forecasting, an additional step has to be taken, that is, derivation of drought events from the forecasted flow time series, e.g. the flow time series is converted into a time series of drought events. In summary, the different approaches that are being used to identify and communicate drought in rivers call for an explicit description of what is being meant. Clearly, different users have diverse needs and these can be accommodated by forecasts of drought indices obtained by different identification approaches as provided in the DEWS.

The purpose of this study, therefore, is firstly to provide a clear overview of the differences between streamflow drought using different definitions (i.e. identification methods) and temporal resolutions, i.e. daily and monthly. This is done through a historic analysis using data from 1990-2018. Differences are illustrated for entire Europe to investigate spatial aspects and some major rivers across different climate regions to study temporal aspects. The historical analysis is innovative because it covers the entire pan-European river network with all its hydrological regimes instead of a single country (Heudorfer and Stahl, 2017; Vidal et al., 2010) or a river basin (Sarailidis et al., 2019) and involves both threshold and standardized identification approaches (drought indices), incl. different temporal resolutions. Secondly, in this study, its implications for forecasting hydrological drought are elaborated using the extreme 2003 drought in Europa as an example, which demonstrates that none of the hydrological drought forecast approaches fits all needs.

The paper is organized as follows: the datasets with observed and ensemble forecasts of streamflow, used in this study, are described in Section 2.1, followed by a description of the methodology to derive the drought indices, i.e. drought identification approaches (Section 2.2), an explanation of presented characteristics, such as the number of drought occurrences (frequency), timing, duration, and deficit volume (Section 2.3). The results are presented and discussed in Section 3. We divided the result section into two parts, that are, drought characteristics analysis using different identification approaches for 1) historical data, and 2) forecasted data of the 2003 drought. Detailed analysis of drought characteristics for both historic and forecasts is provided for the selected river basins. Finally, we conclude the findings in Section 4.

2 Data and Methods

2.1 Data

A state-of-the-art hydrological model, LISFLOOD, was used to simulate the streamflow of rivers across Europe from 1990 to 2018, which was derived from the routed runoff of 5 x 5 km grid cells (van der Knijff et al., 2010; Burek et al., 2013a). We decided to use simulated river flow rather than the observed flow, because sufficiently-long time series of observed flow for a common period covering the whole of the European river network do not exist. The LISFLOOD model was fed by gridded meteorological observations (e.g. precipitation, temperature, relative humidity, wind speed) to obtain daily proxies for observed streamflow data, known as LISFLOOD-Simulation Forced with Observed (SFO). The gridded meteorological observation data were collected from ground observations (>5000 synoptic stations), obtained from the Joint Research Center (JRC) meteorological database, the Global Telecommunication System of the WMO, and high-resolution data received from the National Member States institutions (Pappenberger et al., 2011). The time series of proxy observed streamflow data for each cell at the river network (river grid cell) across Europe were used to derive the streamflow drought following different approaches. Potential evapotranspiration was calculated through the offline LISVAP pre-processor based on the Penman-Monteith equation (van der Knijff, 2008; Burek et al., 2013b). A kinematic wave approach was used for routing the water movement on the river network.

The model was calibrated using time series of observed river streamflow from over 700 calibration stations across Europe. The hydrological skill of the LISFLOOD model expressed by the Kling-Gupta Efficiency (KGE) shows that 42% of all calibration stations score a KGE higher than 0.75, 33% of all stations score a KGE between 0.5 and 0.75, and 25% of all stations score a KGE below 0.5 (Arnal et al., 2019). Although the model was originally developed for operational flood forecasts in the EU under the European Flood Awareness System (EFAS) platform (Thielen et al., 2009; Pappenberger et al., 2011; Cloke et al., 2013), the LISFLOOD model has been tested for drought identification, forecasting and projections (Feyen and Dankers, 2009; Trambauer et al., 2013; Forzieri et al., 2014; Sutanto et al., 2019, 2020a, b; van Hateren et al., 2019). It appears from these studies that the model also performs rather well for drought studies. The model used in this study is the latest version of LISFLOOD that has been implemented in the operational EFAS since 2019 (version 3).

Besides the SFO data, we also used re-forecasted (known as hindcast) time series of streamflow data for the year 2003, as an example of drought forecasts. The European Centre for Medium-range Weather Forecasts System 5 (ECMWF S5) seasonal forecast was used as forcing for the LISFLOOD hydrological model to forecast streamflow at the pan-European scale (Stockdale et al., 2018). The seasonal forecasts are available as daily re-forecast data for each month from day 1 to day 215 (7 months lead-time) for 25 ensemble members (see Sutanto et al., 2020a, for detailed information). In this study, we selected the re-forecast data from 2003, because a severe drought across extended areas in Europe was observed (Fink et al., 2006; Ionita et al., 2017; Laaha et al., 2017).

2.2 Streamflow drought identification

In this study, we employed two well-known drought identification methods, i.e. the threshold drought approach and the standardized drought approach (van Loon , 2015).

2.2.1 The variable and fixed threshold methods

Using both the variable and fixed threshold-based approaches, drought was derived from time series of streamflow data from 1990 to 2018 and re-forecasted data of 2003 to calculate the water deficit in different domains of the water cycle, in our case, it is the streamflow deficit. The threshold approach originates from the theory of runs and is developed based on a pre-defined threshold level (Yevjevich , 1967; Hisdal et al. , 2004). The threshold approach uses an event-based sampling of the flow time series to convert this into a time series of drought events. The drought event starts when the hydrological variable falls below the threshold value and ends when it equals or rises above the threshold value. In this study, we applied two different types of drought threshold approaches, which are the Variable Threshold (VT drought) and the Fixed Threshold (FT drought) on both daily (VTD and FTD) and monthly streamflow data (VTM and FTM). The latter was done to allow a comparison of the VTM and FTM approaches with the Standardized Streamflow Index (SSI, Nalbantis and Tsakiris , 2009; Vicente-Serrano et al., 2012), which uses a monthly temporal resolution. However, the use of threshold approaches on monthly streamflow data to identify monthly drought is not common practice (e.g., Fleig et al., 2006; Peters et al., 2006; Hannaford et al. , 2011; Prudhomme et al., 2014; van Loon , 2015; Marx et al., 2018; Wanders et al. , 2019). To the author's knowledge, only a few studies used monthly data (e.g., Tallaksen et al. , 2009; van Loon et al. , 2019) to derive drought using the threshold method, and this was done only for scientific purposes.

FT uses a pre-defined threshold, which is constant over the year and unique for each river grid cell. The pre-defined VT varies for each day/month and for each river grid cell. The VT method gains more popularity because this method considers seasonality in streamflow (Hannaford et al. , 2011; Prudhomme et al., 2011; van Loon , 2015). For the VT and FT thresholds, we calculated the threshold values using 29 years of monthly streamflow data that were obtained by aggregating daily flow data. Thresholds in this study were derived from the 80th percentile of the streamflow (Q80, flow duration curve), which are the flows that are equaled or exceeded 80 percent of the time. The Q80 was considered as the drought threshold because most of the rivers across Europe are classified as perennial rivers. Moreover, the Q80 threshold lays within the range of the 70th-90th percentile that is commonly used in drought studies (Tallaksen et al. , 1997; Hisdal et al. , 2004; Fleig et al., 2006; Wong et al. , 2011). Using the Q80 means that fewer drought events are identified compared with higher thresholds, e.g. Q70. For the VTM method, the calculated 12 monthly thresholds could be straightforwardly be used in the drought analysis, whereas for the VTD method, the calculated monthly thresholds were firstly assigned as the threshold levels for each day of the respective months. This resulted in a jump between two consecutive months, which showed unrealistic drought behavior. Therefore, as a second step, a 30-day centered moving average (30DMA) smoothing technique was applied to the monthly thresholds, eventually leading to daily thresholds (365 and 366 thresholds for no leap and leap years, respectively) (van Loon et al. , 2012; van Lanen

155 et al., 2013; Beyene et al., 2014). For the FTM and FTD method, we used the same threshold, which is constant throughout the year by definition. In the drought analysis, the same threshold values are applied every year from 1990 to 2018.

The centered 30DMA method was also employed in the historical daily streamflow data to reduce the number of minor droughts (pooling procedure) (Fleig et al., 2006; van Loon and van Lanen, 2012; Sarailidis et al., 2019). This means that we averaged the first 30 days of the SFO data (from 1 to 30 January 1990) to calculate the streamflow on 16 January 1990. For 160 31 January 1990, we averaged the SFO data from 16 January 1990 to 14 February 1990 and so on until 15 December 2018. Missing 30DMA streamflow data from 1 to 14 January 1990 and from 16 to 31 December 2018 were not relevant since we have started drought analyses from the hydrologic year 1991 (from October 1990 to September 1991) to the hydrologic year 2018 (from October 2017 to September 2018). We applied the same hydrologic year for all European rivers. The reason for choosing the same hydrologic year (in our case: 28 years) is to ensure consistency in the analysis at the European level.

165 We also applied the centered 30DMA to the forecast data. To handle the forecast streamflow data at the start of the 215-day forecasts, we averaged 15 days of preceding observed data (SFO) with 15 days of the forecast to predict a possible drought event on the first day. For the second forecast day, we averaged 14 days of preceding observed with 16 days of forecast and so on. For example, the 30DMA forecasted streamflow on 1 August 2003 was obtained from moving averaging the SFO data from 17 July to 31 July 2003 with the forecasted streamflow from 1 August to 15 August 2003 (to predict a possible drought on 170 1 August 2003, lead time one day). Hence, the first 15 forecasted streamflow data from the 215-day time series included some observed flow that increases drought forecast skill for the first 15 days, which will affect possible forecasted drought events at the start of the forecast record using the VTD and FTD. The fusion method was applied to each of the 25 forecast ensemble members. The 30DMA method had not been applied to the monthly streamflow data for both historic period and forecasts. Thus, there is no influence of the SFO data on the monthly drought forecast analysis using the VTM and FTM.

175 2.2.2 The standardized streamflow index

The Standardized Streamflow Index (SSI, Nalbantis and Tsakiris, 2009; Vicente-Serrano et al., 2012) was also used to identify drought in the river. The SSI was calculated using the same theoretical background as the Standardized Precipitation Index (SPI, McKee et al., 1993). The SSI calculation for any river grid cell was based on the monthly streamflow record that is fitted to a gamma distribution, which is then transformed into a normal distribution so that the expected median SSI for the site and 180 desired period is zero. We decided to use the widely selected gamma distribution as general distribution for the whole Europe since it can be used for hydrological forecasting of both high and low flows (Slater and Villarini, 2018). Moreover, none single probability distribution would fit all streamflow time-series across Europe (Vicente-Serrano et al., 2012), in particular, it does not fit all monthly streamflow data in all river grid cells ($n=29,000$). For example, sample properties of streamflow in January might differ from those in August in each of the river grid cells (Tijdeman et al., 2020). In summary, we obtained a gamma 185 distribution parameter set for each river grid cell and month (in total $>348,000$ sets).

A 1-month accumulation period was used in this study (SSI-1 drought). Longer accumulation periods, e.g. SSI with 6-month accumulation period (SSI-6), as it was used in Trambauer et al. (2015) and Barker et al. (2016), was not selected in our study, since streamflow already comprises some catchment memory aspects (delayed flow from groundwater). Nevertheless, we need

to realize that anomalies in the accumulated flow over a longer period (e.g. SSI-6) have relevance for some purposes, such as the management of surface water reservoirs. Negative SSI values indicate a drought event, which means that the streamflow in a certain month is lower than the median streamflow of that month. Four SSI classes are commonly distinguished, which are: 1) mild drought: $0 > SSI \geq -1$, 2) moderate drought: $-1 > SSI \geq -1.5$, 3) severe drought: $-1.5 > SSI \geq -2$, and 4) extreme drought: $SSI < -2$ (Nalbantis and Tsakiris, 2009). In this study, however, we assumed the drought event to start when the SSI-1 falls below -0.84. The use of a threshold -0.84 for SSI warrants a fair comparison between the threshold approaches (Q80) and SSI-1 (SSI < -0.84) (Tijdeman et al., 2020). The above-mentioned gamma distribution parameter sets for SSI-1 and the threshold of -0.84 were used to identify drought events in the historic period (1990-2018) in each of the river grid cells of the pan-European river network.

To forecast a possible SSI-1 drought for a lead-time (LT) of x-month ($x = 1, 2, \dots, 7$ months), we also used the above-mentioned gamma distribution parameters sets. The SSI-1 times series were derived from the forecasted streamflow using these parameter sets (Sutanto et al., 2020a). For example, to forecast SSI-1 using forecasted streamflow initiated on January 2003 with a lead-time of 7-month, we calculate the SSI-1 for January (LT=1), February (LT=2), up to July (LT=7) using the parameter sets from January, February, up to July, respectively. Same parameter sets were applied to each ensemble member to calculate 25 ensembles of SSI-1.

2.3 Drought characteristics

Drought analysis using the threshold methods and the standardized approach shares several common major drought properties or characteristics, which are the number of drought occurrences/frequency (N), drought initiation time or timing (T), and drought duration (D). Another drought characteristics, namely drought deficit volume (DV), can be obtained only by using the threshold methods. The standardized approaches cannot be used to calculate the deficit volume, because it only provides information on the drought severity class (Section 2.2.2) and not about the amount of water that is not available during a drought event (m^3 in our case for streamflow). In this study, the number of drought occurrences, timing, duration, and deficit volume will be calculated using the threshold methods (VTD, FTD, VTM, and FTM). For the SSI-1 the same characteristics will be determined, except the deficit volume.

The number of drought occurrences (N) shows how many drought events occurred: 1) from October 1990 to September 2018 (hydrologic years), and 2) from the starting date of the forecast up to 215 days (7 months) ahead. The timing (T) for drought was determined based on the starting month of each drought event (1: Jan, 2: Feb, ..., 12: Dec) in the time series either in the 28 years (historic analysis) or in the median of the ensembles of 215 days (7 months). If there is more than one drought event in the time series, which is common for the historic data, then we select the timing based on the starting month with the highest frequency. If there is more than two starting months with the same frequency, then we calculate the median value from the selected timings. For example, the month August is selected as drought timing, if months March, August, and October have the same frequency. If there are two starting months detected with the same frequency, then we chose the first timing. Drought duration, expressed in day for VTD and FTD and month for VTM and FTM, is the number of day/month when the streamflow or SSI is continuously below the threshold. If there is more than one drought event, then we average the duration of the events.

The drought deficit volume (only threshold methods) is calculated by summing up the difference between streamflow and the threshold level per day/month over the drought event, expressed in m^3 . For total drought deficit volume, we simply sum up deficit volumes from all drought events (either historic period or forecast period). Obviously, the average deficit volume in a river grid cell, which we use in the historic analysis, equals the total deficit divided by the number of droughts. In case of an ongoing drought in the forecast, e.g. a drought that already started prior to the forecast initiation, we determine the drought characteristics from the first day of the forecast. We do not consider what happened before. In case a drought still has not ended by the end of the forecast period (at day 215 or month 7), we break the drought event by the end of the forecast, meaning that we do not take into account the characteristics of the drought event beyond the forecast period. In addition, we also provide a maximum number of ensemble members indicating drought (N_e) for each forecast initiation as a percentage. For example, for forecasts initiated in July 2003 with $LT=7$ month (from July 2003 to January 2004), we calculate N_e for every LT (1, 2, ..., 7 months), and provide information only for the maximum number of N_e .

2.4 Köppen-Geiger climate classification

The Köppen-Geiger climate classification has been built based on observed global temperature and precipitation data used in Peel et al. (2007). There are four main climate types found in Europe, which are cold (D), arid (B), temperate (C), and polar (E). Each climate type can be classified into several sub-climate types. In our study area, the dominant sub-climate types are Bsk, Csa, Cfa, Cfb, Csb, Dfc, Dfb, Dsa, Dfa, Dsc, and ET (Fig. 1). Six sub-climate types are considered in the streamflow drought analysis across entire Europe, that is, the tundra climate (ET), the warm-summer, humid continental climate (Dfb), the subarctic climate (Dfc), the temperate, oceanic climate (Cfb), the cold, semi-arid climate (Bsk), and the hot summer Mediterranean climate (Csa). The latter two types are clustered in the Mediterranean climate (Med). This means five climate regions that cover over 90% of the European area. In addition to the analysis of streamflow drought in all grid cells of the pan-European river network, four different rivers located in the major climate regimes of Europe were selected. The locations of the selected rivers are as follow: 1) Rhine River near Cologne, Germany, located at 50.9°N and 6.9°E (Cfb), 2) Danube River near Budapest, Hungary, located at 46.9°N and 18.9°E (Dfb), 3) Vuoksi River close to the Finnish-Russian border, located at 61.1°N and 28.8°E (Dfc), and 4) Ebro River near Asco, Spain, located at 41.2°N and 0.6°E (Bsk). The four rivers are indicated by red dots in Figure 1. For detailed information about climate classifications used in the study, see the Köppen-Geiger climate classification presented in Peel et al. (2007).

3 Results and discussion

We present the differences of streamflow droughts identified using different drought identification approaches in two parts. The first part provides results and discusses the historical analysis that consists of the investigation of differences between drought analyzed using different approaches (i.e. drought definitions), in terms of drought characteristics both in over 29,000 river grid cells at the pan European scale, and four selected river basins in more detail (Section 3.1). The second part elaborates the

implication of streamflow drought forecasting using different definitions at the pan European scale and in one of the selected
255 river basins (Section 3.2).

3.1 Historic analysis

3.1.1 Streamflow drought characteristics across Europe

One of the most profound differences among streamflow droughts using different identification approaches is the occurrence
of these events. In a river grid cell, streamflow drought may be absent, occur once, or even more than once in a hydrological
260 year throughout the period 1990-2018. This happens when the streamflow falls below the threshold, which is Q80 (VTs and
FTs) or equal to $SSI < -0.84$ in our study.

The largest deviation between drought occurrences obtained with the five different identification approaches is due to the
temporal resolution. In entire Europe, the variable threshold using daily data (VTD) detects almost 50% more drought events
than when applying monthly data (VTM), i.e. 49.6 and 26.6 events, respectively (Table 1 and 2). The spatial distribution also
265 shows this clearly (Fig. 2a and 2c). The deviation between the daily and monthly resolution for the whole of Europe is smaller
(about 25%) when fixed threshold approaches are applied (FTD: 39.6 and FTM: 28.6 events), see also Fig. 2b and 2d. The data
also show that when a daily resolution is used, the VTD method identifies about 25% more events than the FTD method (Table
1, Fig. 2a, and 2b), whereas deviations are small at the monthly scale (VTM versus FTM, Table 2, Fig. 2c, and 2d). At the
pan-European scale, there are no substantial differences between drought occurrences (<15%) derived with the methods using
270 monthly data (VTM, FTM and SSI-1, Table 2, Fig. 2c, 2d, and 2e).

The maps (Fig. 2a and 2b) show that in about 20% (VTD approach) and 5% (FTD approach) of the pan-European river
grid cells, streamflow drought on average occurs at least twice a year (>60 events). However, in parts of Sweden and Finland,
and southeast Europe, such as Romania, Serbia, and Bulgaria, the occurrence of VTD and FTD droughts does not exceed 30
events during the study period. The highest number of droughts is identified in the temperate oceanic climate (Cfb), whereas
275 the lowest is found in the Mediterranean climate region (Med), irrespective of the identification approach. Clearly, a number
of events vary amongst identification methods, for example, the range for the Cfb and Med climates is 30.4-57.8 and 22.6-41.0
events, respectively (Table 1 and 2).

Minor drought events are assumed to be the main reason for the high occurrence of VTD and FTD droughts in the major
European rivers (>60 events), compared to VTM and FTM droughts (Fig. 2a, 2b, 2c, and 2d). To prove our hypothesis, we
280 plotted the percentage of VTD drought events that have duration of shorter than 30 days (Fig. A1). Here, it can be seen that
many rivers in the west and east Europe (Cfb and Dfb climates), as well as, the mountainous regions in Norway (Dfc and ET),
experience lots of minor drought events (>60% of total number, and even more, up to almost 100% in a few rivers indicated by
red color). Mediterranean and Dfc climate regions (Sweden and Finland), in general, show a smaller number of minor drought
events (~30% of total), meaning that drought events in these regions (Fig. 2a) are caused by droughts that have a long duration.
285 This will be discussed later (Fig. A2).

To investigate the timing of streamflow drought, we present the month when drought mostly starts in each grid cell of European rivers (Fig. 3). The timing was determined for each drought event in the period October 1990 to September 2018. Figure 3 indicates that, as expected, there is a strong relation between streamflow drought timing in the rivers and the Köppen-Geiger climate regions across Europe (compare Fig. 1 and 3). This also differs among drought identification methods. In general, the fixed threshold methods (FTD and FTM) detect earlier drought (Table 1 and 2) than the fixed threshold methods (VTD and VTM), except in many rivers located in the humid continental climate (Dfb). Rivers located in cold climate regions (Dfb and Dfc), such as northern and eastern Europe, and the Alps, experience streamflow drought events in late winter and early spring (March-April) when the daily variable threshold method (VTD) is applied (Fig. 3a, Table 1), and later when monthly data (VTM) are used (May-July, Fig. 3c, Table 2). In addition to below normal precipitation and above normal evaporation (classical rainfall deficit drought), drought in cold regions also depends on the length of the frost period and the timing of snow incidents, accumulation, and melting (cold snow season drought) (van Lanen et al., 2004; Pfister et al., 2006; van Loon and van Lanen, 2012). A warm snow season drought may also occur during spring or summer, associated with no snow occurrence during winter or earlier snowmelt than normal (van Lanen et al., 2004; van Loon et al., 2010). This causes an early peak in streamflow, resulting in lower streamflow in late spring and summer. In the warmer climates (Cfb and Med) droughts start later (mostly July-October) than in the colder regions. However, there is a difference between variable and fixed threshold approaches, i.e. FT droughts largely begin earlier (July-August, Fig. 3b and 3d) than the VT droughts (September-October, Fig. 3a and 3b, Table 1 and 2). The start of SSI-1 drought in most climates is closest to VTM droughts (Fig. 3e, 3c, and 3d, Table 2).

The average duration of the droughts (Fig. A2) is negatively correlated with the number of droughts when using the threshold methods (Fig. 2). We have seen that applying methods using daily data result in more drought occurrences than those that use monthly data. Hence, the average drought duration of events is connected with the temporal resolution of the methods. We have seen that droughts obtained with methods fed by daily data (Fig. 2a and 2b) are shorter than those applying monthly data (Fig. 2c and 2d). For instance, for the whole pan-European river network, VTD droughts are about 60% shorter than VTM droughts (44.6 days and 2.4 months/73 days, respectively, Table 1 and 2). For the FT drought, the following average drought duration was found: FTD 56.0 days and FTM 2.5 months/74 days, implying that the FTD droughts are about 30% shorter than FTM events. We also observed that rivers in the Cfb climate have the highest number of droughts and those in the Mediterranean climate region have the lowest number of droughts, implying that the average drought duration in the Cfb climate is shorter (36.4 and 47.2 days, Table 1, and 1.9 months/57 days, and 2.2 months/66 days, Table 2) than in the Mediterranean region (56.3 and 68.4 days, Table 1, and 2.9 months/87 days, and 2.7 months/81 days, Table 2), see also Fig. A2a, A2b, A2cs and A2d. The average drought duration estimated with the SSI-1 approach is close to both the VTM and FTM methods (Fig. A2c, A2d, and A2e). Differences in average drought duration amongst methods using monthly data for the whole of Europe are around 10% (Table 2).

The average drought deficit volume that has been detected by the different drought identification methods is to some extent linked to the temporal resolution of the methods. For example, for the whole of Europe, we found higher average drought deficits with the approaches using monthly data (VTM: 1,371 and FTM: 1,211 m³) than those fed by daily data (VTD: 919

and FTD: 913 m³), indicating about 25-30% higher drought deficit volumes (Table 1 and 2). Plotting average drought deficit volume across European rivers (Fig. A3), in general, shows higher deficit volumes for the bigger rivers in central and north Europe (except coastal areas), which is partly caused by not standardizing the deficit volumes. Hence, the analysis of the drought deficit volume using different identification approaches is more meaningful, if we summarize the results for each climate region (Table 1 and 2) or for selected river grid cells (Section 3.1.2). The highest deficit volume is found in the humid continental climate (Dfb) and the lowest in the Mediterranean climate, irrespective of the identification method (Table 1 and 2), although the deficit volumes differ per method.

The pan-European analysis of the river network (Table 1 and 2, Fig. 2, 3, A2, and A3) evidently demonstrates that drought characteristics (occurrence, timing, average duration, average deficit volume) determined by commonly applied identification methods (variable threshold versus fixed threshold, daily versus monthly resolution, threshold versus standardized approach) are different. The differences are also dependent on the climate region.

3.1.2 Drought occurrences in selected rivers and periods

For a more detailed analysis of the differences of streamflow droughts derived from different approaches, as illustrated above for the whole pan-European network, we investigated four rivers situated in main climates across Europe (Fig. 1) for particular periods. The pan-European analysis focused on the spatial aspects of the differences between the drought identification methods, whereas the detailed analysis of the four selected rivers emphasizes the temporal aspects. Figure 4 and 5 show for some selected years a detailed analysis of drought in the rivers. The proxy observed flow (30DMA hydrograph) of the period 2000-2004 from the Rhine River in combination with the daily threshold methods (VTD and FTD) clearly show that streamflow drought mainly occurred from summer 2003 to January 2004 (Fig. 4a). The year 2003 is one of the most notable drought years in Europe (Fink et al., 2006; Ionita et al., 2017; Laaha et al., 2017). During wet years, e.g. from 2000 to 2002, there were no streamflow drought events identified (both VTD and FTD). The difference in drought occurrence in the Rhine River in the selected 5-year period between the daily methods is small, for example, there are a few minor droughts detected (early 2003 summer, December 2004) with the VTD, whereas these were not found with the FTD. The deficit volume of the drought event in summer 2003 was clearly larger for the FTD than of the VTD. In the winter of 2003-2004, the opposite happened (Fig. 4a). The different identification approaches using monthly data (VTM, FTM, and SSI-1) also detected the 2003 drought as the major event in the 2000-2004 time series (Fig. 5a), which terminated in October due to some precipitation. This precipitation had a more marked effect on the SSI-1 drought than on the VTM and FTM droughts. Some minor drought events were identified in autumn and winter 2003 with all three methods, although the timing was different. For instance, the SSI-1 drought was later than the FTM drought (Fig. 5a).

A difference between drought identification approaches using daily and monthly drought methods is clearly seen in the Danube River (Fig. 4b and 5b). Many minor drought events were recognized using daily data, that is, in winters from 2000 to 2002, spring 2003 and 2004 for FTD, and in spring 2003, spring 2004, summer 2004, and winter 2004/2005 for VTD. In contrast, minor drought events in winter 2001/2002 and in spring 2003 did not occur if we applied drought identification approaches using monthly data (FTM and VTM, respectively, Fig. 5b). Figure 4b and 5b demonstrate that during rather wet

355 years (the year 2000-2002), no VTD, VTM, and SSI-1 droughts were observed. The VT and SSI-1 approaches take into account seasonality in their analyses. Similar to the Rhine River, in the Danube, a major drought event in 2003 was identified using all approaches (Figure 4b and 5b).

In the Vuoksi River, which is located in the cold climate region (Dfc, Fig. 1), all drought identification approaches show more or less similar drought occurrences (Fig. 4c and 5c). The FT approaches, both at the daily and monthly scale, detect slightly
360 more events than those that consider seasonality (VT methods and SSI-1). Two multi-year drought events (Tallaksen and Van Lanen, 2004) were detected in 1999-2000 and 2002-2003 with all drought approaches. The main reason for this is that there is only a small difference between daily and monthly streamflow. The presence of water bodies, such as lakes, causes daily streamflow not to be highly variable in short term. This attenuates and damps the streamflow response to the driving force, i.e. precipitation, incl. snowmelt, and is thus driven by longer-term previous hydrological conditions (Pechlivanidis et al., 2020).

365 In the first decade of the 21st Century, climate variability in the Mediterranean regions caused different wet/dry periods compared to the rest of Europe. In contrast to the severe 2003 drought in central and west Europe, the most severe droughts in, e.g. Catalonia (Spain), were observed from 2005 to 2008 (Martin-Ortega et al., 2012; March et al., 2013), which is illustrated by the streamflow of the Ebro River (Fig. 4d and 5d). Pronounced FTD droughts occurred every year in the period 2005-2009, whereas only minor VTD drought occurred in the last year (Fig. 4d). Using monthly instead of daily streamflow data reveals
370 a similar pattern (Fig. 5d), i.e. no VTM droughts from summer 2008 to 2009, while these happened in all summers according to the FTM method. The droughts in 2005-2007 also illustrate differences in timing between VT and FT methods, both at the daily and monthly scale, i.e. limited coinciding periods (orange-shaded in Fig. 4d and 5d). The SSI-1 droughts follow the pattern of VTM droughts. A multi-year drought event from summer 2007 to spring 2008 was identified with all approaches, although duration is different (e.g. FT droughts, FTD and FTM, lasted markedly longer than VT droughts, VTD and VTM, as
375 well as SSI-1 drought). Another major drought event in the Ebro was observed in 2005. In contrast to the 2007-2008 drought in this year, the Ebro River experienced considerably longer VTD, VTM, and SSI-1 droughts than FTD and FTM droughts.

Above we explained differences in drought characteristics derived from different identification methods for the four selected rivers for a 5-year period. A summary of the outcome from all five drought identification methods for the four selected rivers and all hydrological years (1991-2018) is presented in the Supplementary Material (Supplementary Table S1 and Table S2).

380 **3.1.3 Summary of differences between drought identification approaches**

The more detailed drought analysis of the four selected rivers in the previous section and the broader analysis of the pan-European river network (Section 3.1.1, Table 1 and 2) show that the FTD approach identifies a lower number of drought events than the VTD. On the other hand, when monthly approaches are used to detect drought, the FTM approach results in slightly more droughts than the VTM. Clearly, relative differences are smaller than for the daily resolution. Sarailidis et al.
385 (2019) found for the Yermasoyia catchment (Cyprus) a smaller number of droughts both at the monthly and daily resolution when applying the fixed threshold instead of the variable threshold, which is in line with our daily results (FTD versus VTD). Overall, early droughts were identified using the fixed threshold methods, irrespective of the temporal resolution (FTD and FTM). Rivers located in the Dfb climate, however, have later FT droughts than the VT droughts. The FTD identifies longer

droughts than the VTD, whereas the differences in average duration when using the monthly resolution (FTM and VTM) are small. Our findings on drought duration at the daily time scale are also found by Heudorfer and Stahl (2017) in a study dealing with four case catchments in Germany. In the pan-European analysis (Table 1 and 2), we found that the drought deficit volume obtained with the VT methods (VTD and VTM) is slightly higher than with the FT methods (FTD and FTM). This is confirmed by a study done by Sung and Chung (2014) for the Seomjin River basin in Korea. Not all four selected rivers follow this pattern, for instance, in the Rhine and Danube, application of the FT methods results in higher deficit volumes than the VT methods (Supplementary Table S1 and S2), which is also found by Sarailidis et al. (2019) in the Yermasoyia catchment. Obviously, individual rivers may deviate from the general pattern. Our generic finding that the streamflow drought characteristics (frequency, duration, timing) depend on the identification method is in line with the observations made by Vidal et al. (2010), who for streamflow drought in France also concluded that the identification method, although different (only standardized-based indices at multiple time scales) from our study, is crucial.

3.2 Implication of different drought identification approaches to forecast streamflow drought

So far, this paper has focused on a historical drought analysis using different identification approaches, which creates a base for the implications of these findings for the forecasting of streamflow drought. First, we illustrate the implications at the pan-European scale with focus at the spatial aspects followed by a more detailed temporal analysis for the Rhine River, as one of the four selected rivers above. The 2003 drought is used as an example.

3.2.1 Forecasting streamflow drought characteristics across Europe

Consequences of using different drought identification approaches to forecast streamflow drought characteristics across Europe are described in this section. The forecast initiated in the first of July 2003 (median of 25 ensemble members) for 7 months ahead (up to January 2004, see Section 2.3 for the calculation of drought characteristics using forecast data) is used for illustration. We show the forecasted drought duration and timing here (Fig. 6 and 7, respectively), while the forecasted frequency of drought occurrences and drought deficit volumes are provided in appendix B.

Figure 6 shows the forecasted average drought duration in Europe using the forecast initiated in July 2003 for a 7-month lead time (July 2003-Jan 2004). Longer drought duration is forecasted in many European rivers using the FT approaches (FTD and FTM, Fig. 6b and 6d) than the VTs (VTD and VTM, Fig. 6a and 6b), up to 60 days/2 months, which for the daily resolution was expected based on the historic analysis (up to ~20%, Table 1). The SSI-1 approach forecasts similar drought duration to VTM (Fig. 6e and 6c). Using the VT and SSI-1 approaches, drought was forecasted to last on average 40 days or ~1 month in the period July 2003-Jan 2004 in many European rivers. The FT methods predict an average duration of 120 days or ~4 months. Rivers located in Eastern European countries, such as in Belarus, Ukraine, and Romania were predicted to have a long drought duration in the above-mentioned period according to all approaches (up to 200 days, 7 months, Fig. 6). This region (the eastern part of Europe) is identified as an area suffering from severe hydrological drought hazards, where the frequency of drought is small compared to other European regions, but with the drawback that droughts last long (Sutanto and Van Lanen, 2020). The forecasted average drought durations in the Cfb, Dfc, and Mediterranean climates using the FT approaches are

around 100 days for FTD and 3-4 months for FTM (Fig. 6b and 6d), which is almost threefold longer than obtained with the VT approaches.

Figure B1 presents the forecasted number of drought events from July 2003 to January 2004 (LT=7) derived from different drought approaches. In general, the VT (VTD and VTM) and SSI-1 approaches forecast that at least one drought event would occur in lots of river grid cells in Europe (~80%, Fig. B1a, B1c, and B1e), which is lower than the number of droughts forecasted with the FT approaches (~90%, Fig. B1b and B1d). These differences in drought frequency between identification approaches are not uniformly distributed over Europe. For instance, in the Cfb and Dfb climates, the opposite is found, that is, VT methods forecast higher drought frequency than FT methods. The differences in the number of drought occurrences between the identification approaches highlight the importance of considering whether seasonality should be taken into account (VT and SSI-1 droughts) in the forecasting, or not (FT droughts).

The forecasted drought start in the period July 2003-Jan 2004 (month that the first drought appears, see Section 2.3 for the determination of the start month/timing) using the VT approaches and SSI-1 is, in general, later than of the FT approaches, except in the cold regions, such as Dfc and ET (Fig. 7). In the Cfb, Dfb, and Mediterranean climates, the VT and SSI-1 approaches predict the drought timing in September to December (Fig. 7a, 7c, and 7e), while the start of the forecasted FT droughts is earlier, i.e. July to September (Fig. 7b and 7d). It is vice versa for the Dfc region (Sweden and Finland), where forecasted VT and SSI-1 droughts are earlier (July) than FT droughts (December and January). Higher drought deficit volume than 2000 m³ is predicted for the period July 2003-Jan 2004 in many European rivers using the FT approaches than those predicted with the VTM ones (Fig. B2). An exception is seen for some big rivers flowing through Hungary, Ukraine, Romania, and Bulgaria. Both VT and FT drought have a high deficit volume predicted there, because of the long drought durations (Fig. 6).

3.2.2 Forecasted drought characteristics for the Rhine River

In the previous section we have dealt with streamflow forecasting for the pan-European river network that mainly focusses on spatial aspects. Here, we concentrate more on the temporal aspects, and use the Rhine River as an example. Figure 8 illustrates the proxy observed and forecasted 25 ensemble streamflows (grey shaded area) in the Rhine River (location 1, Fig. 1) initiated in April and July 2003 for 7 months ahead and the forecasted median ensemble streamflow (purple line) using all drought identification methods. In addition, the forecasted droughts in streamflow are given (shaded areas below thresholds). We choose the 7-month forecast initiated in April 2003 (Fig. 8a, 8c, and 8e) covering spring, summer, and autumn to explore if the forecasts obtained with different identification methods are able to predict drought that occurred in summer 2003. July 2003 was chosen because streamflow drought based on observations (SFO) was starting in this month (see Fig. 4a). VTD and FTD drought forecasts done in April using the median ensemble identify a minor drought that occurred in April (orange area) and from August to October only for FTD (red areas), i.e. the purple line is below the blue (VT) and the red line (FT) (Fig. 8a). The forecast done in April (Fig. 8a) also shows that some dry ensemble members predict two long-lasting droughts, both for FTD and VTD, that is, from mid April to early June, and from August to the end of the forecast record (October). On the other hand, some other ensemble members do not predict any drought at all in the April-October forecast record. VTD and

FTD drought forecasts done in July using the median ensemble identify minor drought events that would occur in July and November (orange areas), whereas a major FTD drought would happen from the end of July to the end of October (Fig. 8b). In general, the FTD method forecasts more drought events in 2003 than the VTD (Fig. 8a and 8b).

460 In contrast to the daily threshold approaches, drought forecasts done in April 2003 using the monthly drought identification approaches, VTM, FTM, and SSI-1, do not forecast a drought event that would occur in summer (Fig. 8c and 8e, see Fig. 5a for observed drought). A minor drought event is predicted with the FTM method by the end of the forecasts, which is September (red shaded area). Monthly drought forecasts done in July 2003 predict a FT drought from August to the end of September (Fig. 8d). This indicates that all the forecast approaches miss the ongoing drought event in July, as it was observed (Fig. 5a). The VTM approach, on the other hand, does not predict any drought event, whereas the SSI-1 forecasts a minor drought event 465 in the beginning of July, but no other droughts later in 2003 are forecasted (Fig. 8f).

In general, drought events (i.e. occurrence) can relatively be well forecasted using the median of ensemble members, but this holds to a lesser extent to other drought characteristics, such as severity, duration, and deficit volume. Additional metrics than the median, such as 25th and 10th percentiles taken from the ensembles, must also be considered for drought forecasting, as done by Sutanto et al. (2020a). Figure 8 clearly demonstrates that the observed streamflow is placed in between the lowest 470 ensemble member and the ensemble median during a severe drought event, as the 2003 drought. Irrespective of the skill, the forecasts of the drought for the Rhine River show that predicted drought characteristics very much depend on the identification method, incl. the temporal resolution (daily versus monthly).

For a better overview of forecasted drought characteristics in the Rhine River than in Figure 8, we summarize all 7-month forecast results done from January 2003 to December 2003 in Table 3 for daily drought approaches (VTD and FTD) and in 475 Table 4 for monthly drought approaches (VTM, FTM, and SSI-1) using the median of the ensemble members. This implies that not only the April and July forecasts are considered, as done in Figure 8, but also forecasts done in all the other months of 2003, meaning that the December forecast covers the first six months of 2004. The forecasts initiated in January, February, and March using daily data (Table 3) did not predict any drought event in 2003 (except for some ensemble members, $N_e > 0$). Droughts were predicted not earlier than forecasts issued in April. In April, three minor VTD droughts and nine minor FTD droughts were 480 predicted to occur with average drought duration of 2.7 and 6.1 days, respectively. The timing shows that droughts will start in April (VTD) and September (FTD). For drought events forecasted in April using the VTD method, the maximum number of ensemble members (N_e) foreseeing these three minor drought events in the period April-October is 88% (22 members out of 25 fall below the threshold). The FTD method shows the same number of members (22 members, 88%). The number of ensemble members in drought (N_e in %) can be used as a measure for drought forecast uncertainty or the forecast confidence 485 level. The higher the percentage, the more likely the drought will occur (higher confidence level). In our case, VTD and FTD droughts were predicted to occur in the Rhine River with a high confidence level ($N_e=100\%$) starting from July until at least the end of the year 2003. The forecast issued in July 2003 predicts the highest number of VTD drought events up to 14 events with an average duration of 2.8 days. The FTD method shows a lower drought frequency (9 events) but with a longer average duration (12.7 days). The longest average drought duration was predicted by the VTD forecast initiated in October (24 days) 490 and in June for FTD (28.7 days). For the drought deficit volume, the highest water deficit was predicted using forecast initiated

in October and December for VTD (4,502 m³ and 10,654 m³, respectively) and in August and December for FTD (5,877 m³ and 14,720 m³, respectively).

The monthly drought approaches, on the other hand, show different results from the daily approaches for most of the characteristics (compare Table 3 and 4). The FTM method predicts one drought event in each of the forecasts initiated from April to December with medium to high confidence ($Ne > 50\%$). The VTM method foresees one or two events from the May forecast onwards with a medium to high confidence level ($Ne > 50\%$). The SSI-1 method starts predicting droughts two or three months later than the threshold approaches. The longest predicted VTM drought (two months) and most severe (total deficit volume: 10,210 m³) was done by the forecast initiated in September. The longest FTM drought was predicted (up to 4 months) with the forecast initiated in August. This FTM drought also has the highest drought deficit volume (32,883 m³). The analysis of the forecasts from January to December for the Rhine River (Table 3 and 4) clearly shows that forecasted drought characteristics depend on the identification method.

In this study, we highlight the occurrence of minor droughts derived with the daily threshold methods (VTD and FTD) as a reason for the high drought frequency (Fig. 2a, Fig. 2b, Fig. 4, Fig. 8, Fig. A1, Fig. B1, Table 1, and Table 3). A high number of VTD minor droughts with short duration and small deficit volume may disturb drought analysis. Tallaksen et al. (1997) and Fleig et al. (2006) suggest several pooling procedures to reduce the number of minor droughts, such as applying the inter-event time method (IT-method), the moving average procedure (used in this study), and the sequent peak algorithm (SPA). They state that minor droughts are automatically filtered out when the moving average procedure is applied. In our study, however, this only happens to a certain extent. As expected, when we would not have applied the 30DMA, the number of drought occurrences would have been higher, i.e. in this case by a factor of three (Fig. 2a and A4).

In addition to these pooling techniques, the exclusion of drought events with duration shorter than a given number of days is recommended (Jakubowski and Radczuk, 2004; van Loon et al., 2012). For example, van Loon et al. (2012) excluded droughts that have duration less than three days, van Loon and van Lanen (2012) excluded droughts that have duration fewer than 15 days, and some studies excluded droughts that have duration less than five days (Hisdal et al., 2004; Birkel, 2005; Fleig et al., 2006). In the end, the choice to exclude drought events shorter than a particular number of days to avoid minor droughts in the drought analysis, is a matter of subjectivity. We showed in our analysis that if we would have excluded drought <30 days (Fig. A1), the number of drought occurrences in most of the European rivers would decrease by 60% (Section 3.1.1). In this study, although we excluded many minor drought events by applying moving average procedures, which is the 30DMA for drought analyses (Section 2.2.1), minor drought events are still there (Fig. A1). In this study, we did not apply pooling procedures, as mentioned above, besides the 30DMA.

520 4 Conclusions

Streamflow drought forecasting may use different identification approaches to detect drought events, i.e. threshold and standardized approaches. This study presents a drought analysis using simulated historical streamflow data from the pan-European rivers network. It consists of almost 30,000 river grid cells and is located in different climates across Europe. We applied

commonly identification approaches, which are the daily Variable Threshold (VTD), the daily Fixed Threshold (FTD), and the Standardized Streamflow Index (SSI-1) that uses aggregated streamflow over a month. In addition, we also provide results derived from monthly threshold approaches (VTM and FTM) for a fair comparison with the SSI-1 drought. These approaches generate several drought characteristics, namely frequency, duration, timing, and deficit volume (latter not for SSI-1). The largest difference amongst the drought identification approaches comes from the temporal resolution. When using the same drought identification approach (variable or fixed threshold methods), but using different data aggregation levels (daily versus monthly), the daily methods evidently generate more drought occurrences. The daily variable threshold method (VTD) detects almost twice as many drought events as the monthly method (VTM). The FTD also identifies more drought events than the FTM, but deviation is smaller (about 25%). Minor droughts shorter than 1 month are the main reason for the higher number of drought occurrences identified by the daily threshold methods (VTD and FTD). The frequency of drought occurrences derived from the VTD approach is higher than obtained with the FTD, whereas the differences amongst methods using monthly data (VTM, FTM and SSI-1) is rather small (<15%).

Identification of streamflow droughts using different methods also affects timing, i.e. the month in which the drought starts. Differences are also controlled by climate regions. In general, the fixed threshold methods (FTD and FTM) detect earlier drought than the fixed threshold methods (VTD and VTM), except many rivers the humid continental climate (Dfb). Rivers located in cold climate regions (ET, Dfb and Dfc) experience streamflow drought events in late winter and early spring (March-April) when the daily variable threshold method (VTD) is applied, and later when monthly data (VTM) are used (May-July). When using the fixed threshold methods not such clear pattern in the start of the drought in the cold climates was found (FTD: February-June, and FTM: February-July). Drought in the Mediterranean climate mostly starts late, in late summer or autumn (August-October), irrespective of the identification method. The start of SSI-1 droughts is closest to VTM droughts. Average drought duration for the threshold methods is more controlled by the number of occurrences (i.e. negatively correlated). This implies that the drought duration obtained with the daily threshold methods (VTD and FTD) is shorter than derived from the monthly methods (VTD and VTM), and that the FTD droughts last longer than VTD droughts. In addition, the methods using daily data produce drought events with lower drought deficit volumes (25-30%) than the methods fed with monthly data. It is important to note that the findings for the whole pan-Europe river network are generic. Individual rivers, as illustrated with some selected rivers, may deviate from the general pattern.

The different drought identification approaches were also applied to streamflow forecasting with the 2003 drought as an example, which yielded similar conclusions to the historical analysis. The forecasted average drought duration across Europe done in July 2003 clearly differs between the daily and monthly approaches, in particular the VTM and SSI-1 predict lower average duration for the upcoming 7 months. The seasonal forecasts issued each month in 2003 for the Rhine River supports the substantial differences in forecasted drought characteristics amongst methods using daily or monthly data and between variable and fixed threshold methods. The differences in drought frequency, average duration, timing, and deficit volumes between VT droughts (incl. SSI-1) and FT droughts highlight the importance of whether end-users of drought forecasts should take seasonality into account or not. Moreover, the temporal resolution of drought identification, that is, the use of daily or monthly data, is critical to consider. When the drought deficit volume is required, then the standardized approach (SSI) cannot

be selected. The choice of the drought identification method when forecasting streamflow drought, in the end, lies in the
560 end-users specific requirements and decisions, and there is no one drought identification approach that fits all needs. For this
particular reason, the European DEWSs, such as the European Drought Observatory (EDO, Sepulcre-Canto et al., 2012) and
the Anywhere DEWS (ADEWS, Sutanto et al., 2020a) forecast both standardized-based and threshold-based drought indices.

Our study, both the historical analysis and the forecasting, clearly shows that streamflow droughts obtained from different
drought identification approaches (variable threshold (daily versus monthly), fixed threshold (daily versus monthly), and stan-
565 dardized index) differ in terms of their drought characteristics. Often scientists have analyzed and provided streamflow drought
forecasts without clearly defining the identification method. This created misconceptions, miss-citations, and confusion among
the academic community (authors, reviewers, editors), operational weather and water services, as well as end-users, which con-
sider drought forecast products and associated terminology as interchangeably. Our study recommends scientists, developers
of Drought Early Warning Systems, and end-users to clearly agree among themselves, preferable in a co-design phase, upon a
570 sharp definition of which type of streamflow drought is required to be forecasted to mitigate the impacts of drought. Obviously,
Drought Early Warning Systems also can include more than one drought identification method, as illustrated by Sutanto et al.
(2020a). Then the end-user can decide in the end, which forecast product is most adequate based upon the provided description
of the identification method and product.

Data availability. The streamflow EFAS data are accessible under a COPERNICUS open data license (<https://doi.org/10.24381/cds.e3458969>).
575 In this study, we used EFAS system version 3. The SSI-1 analyzed using the SFO data and re-forecasts are available online in the 4TU Centre
for Research Data with doi:10.4121/13056071.v1.

Appendix A: Drought characteristics obtained from historical data

Appendix A includes drought characteristics obtained using proxy observed (SFO) data from 1990 to 2018. In Figure A1, we
present the number of minor drought occurrences that have duration less than 30 days. Streamflow drought was identified using
580 the VTD approach. Figure A2 and A3 show the average duration of streamflow drought and average drought deficit volume in
the European rivers identified with different drought identification approaches, namely the VTD, FTD, VTM, FTM, and SSI-1.
Figure A4 illustrates the number of drought occurrences in European rivers from October 1990 to September 2018 (28 years)
identified using the VTD approach without smoothing, i.e. applying the 30DMA method.

Appendix B: Forecasting drought occurrence and deficit volume

585 Appendix B describes forecasted drought characteristics in major European rivers obtained from the forecast initiated in July
2003 for 7 months ahead (up to January 2004). Drought characteristics were derived using different drought identification
approaches, namely the VTD, FTD, VTM, FTM, and SSI-1. Figure B1 and B2 show forecasted drought occurrences and
forecasted average drought deficit volume, respectively.

Author contributions. S.J.S and H.A.J.V.L conceived and implemented the research. Data analyses, model output analyses, and all figures
590 have been performed by S.J.S. S.J.S and H.A.J.V.L wrote the initial version of the paper and equally contributed to interpreting the results,
discussion, and improving the paper.

Competing interests. The authors declare no competing financial and/or non-financial interests in relation to the work described.

Acknowledgements. The research is supported by the ANYWHERE project (Grant Agreement No.: 700099), which is funded within EU's
Horizon 2020 research and innovation program www.anywhere-h2020.eu. The streamflow data came from the EFAS computational center,
595 which is part of the Copernicus Emergency Management Service (EMS) and Early Warning Systems (EWS) funded by framework contract
number 198702 of the European Commission. We thank Fredrik Wetterhall (ECMWF) for providing the EFAS data and two anonymous
reviewers that helped to substantially improve the paper. This research is part of the Wageningen Institute for Environment and Climate
Research (WIMEK-SENSE) and it supports the work of UNESCO EURO FRIEND-Water and the IAHS Panta Rhei program of Drought in
the Anthropocene.

600 References

- Arnal, L., Asp, S.-S., Baugh, C., De Roo, A., Disperati, J., Dottori, F., Garcia, R., Garcia-Padilla, M., Gelati, E., Gomes, G., Kalas, M., Krzeminski, B., Latini, M., Lorini, V., Mazzetti, C., Mikulickova, M., Muraro, D., Prudhomme, C., Rauthe-Schoch, A., Rehfeldt, K., Salamon, P., Schweim, C., Skoien, J.O., Smith, P., Sprokkereef, E., Thiemig, V., Wetterhall, F., and Ziese, M.: EFAS upgrade for the extended model domain-technical documentation. Publications Office of the European Union, Luxembourg, EUR 29323 EN (ISBN 978-605 92-79-92881-9), <https://doi.org/10.2760/806324>, 2019.
- Arnal, L., Cloke, H. L., Stephens, E., Wetterhall, F., Prudhomme, C., Neumann, J., Krzeminski, B., and Pappenberger, F.: Skilful seasonal forecasts of streamflow over Europe?, *Hydrol. Earth Syst. Sci.*, 22, 2057–2072, <https://doi.org/10.5194/hess-22-2057-2018>, 2018.
- Barker, L. J., Hannaford, J., Chiverton, A., and Svensson, C.: From meteorological to hydrological drought using standardised indicators, *Hydrol. Earth Syst. Sci.*, 20, 2483–2505, doi:10.5194/hess-20-2483-2016, 2016.
- 610 Bell, V. A., Davies, H. N., Kay, A. L., Brookshaw, A., and Scaife, A. A.: A national-scale seasonal hydrological forecast system: development and evaluation over Britain, *Hydrol. Earth Syst. Sci.*, 21, 4681–4691, 2017.
- Belayneh, A., Adamowski, J., Khalil, B., and Ozga-Zielinski, B.: Long-term SPI drought forecasting in the Awash River Basin in Ethiopia using wavelet neural network and wavelet support vector regression models, *Journal of Hydrology*, 508: 418–429, <https://doi.org/10.1016/j.jhydrol.2013.10.052>, 2014.
- 615 Beyene, B. S., Van Loon, A. F., Van Lanen, H. A. J., and Torfs, P. J. J. F.: Investigation of variable threshold level approaches for hydrological drought identification, *Hydrol. Earth Syst. Sci. Discuss.*, 11, 12765–12797, <https://doi.org/10.5194/hessd-11-12765-2014>, 2014.
- Birkel, C.: Temporal and Spatial Variability of Drought Indices in Costa Rica, Master's thesis, Albert-Ludwigs-Universität, Freiburg, Germany, 2005.
- Burek, P., van der Knijff, J., and Roo, A. D.: LISFLOOD distributed water balance and flood simulation model, JRC Tech. Report, 620 <https://doi.org/10.2788/24719>, 2013a.
- Burek, P., van der Knijff, J., and Ntegeka, V.: LISVAP Evaporation Pre-processor for the LISFLOOD water balance and flood simulation model, JRC Tech. Rep., EUR26167EN, doi:10.2788/26000, 2013b.
- Changnon, S. A.: Detecting drought conditions in Illinois, Champaign Circular 169, Illinois State Water Survey, 36 pp., [ISWS/CIR-169/87], 1987.
- 625 Clark, M. P., and Hay, L. E.: use of medium-range numerical weather prediction model output to produce forecasts of streamflow, *Journal of Hydrometeorology*, 5, 15–32, 2004.
- Cloke, H., Pappenberger, F., Thielen, J., and Thiemig, V.: Operational European flood forecasting, in: *Environmental Modelling: Finding Simplicity in Complexity*, 2nd edn., Wainwright, J. and Mulligan, M. (Eds.). John Wiley and Sons, Ltd, Chichester, UK, <https://doi.org/10.1002/9781118351475.ch25>, 2013.
- 630 Day, G. N.: Extended Streamflow Forecasting Using NWSRFS, *Journal of Water Resources Planning and Management*, 111(2), 157–170, 1985.
- Ding, Y., Hayes, M., and Widhalm, M.: Measuring economic impacts of drought: a review and discussion, *Disaster Prevention and Management*, Vol. 20 No. 4, pp. 434–446, <https://doi.org/10.1108/09653561111161752>, 2011.
- Duan, Q., Pappenberger, F., Wood, A., Cloke, H. L., and Schaake, J. C.: *Handbook of Hydrometeorological Ensemble Forecasting*, Springer, 635 <https://doi.org/10.1007/978-3-642-39925-1>, 2019.

- Dutra, E., Pozzi, W., Wetterhall, F., Di Giuseppe, F., Magnusson, L., Naumann, G., Barbosa, P., Vogt, J., and Pappenberger, F.: Global meteorological drought – Part 2: Seasonal forecasts, *Hydrol. Earth Syst. Sci.*, 18, 2669–2678, doi:10.5194/hess-18-2669-2014, 2014.
- Feyen, L., and Dankers, R.: Impact of global warming on streamflow drought in Europe, *J. Geophys. Res.*, 114, D17116, doi:10.1029/2008JD011438, 2009.
- 640 Fink, A. H., Brücher, T., Krüger, A., Leckebusch, G. C., Pinto, J. G., and Ulbrich, U.: The 2003 european summer heatwaves and drought-synoptic diagnosis and impacts, *Weather, Royal Meteor. Soc.*, 59, 209–216, doi:10.1256/wea.73.04, 2006.
- Fleig, A. K., Tallaksen, L. M., Hisdal, H., and Demuth, S.: A global evaluation of streamflow drought characteristics, *Hydrol. Earth Syst. Sci.*, 10, 535–552, 2006.
- Forzieri, G., Feyen, L., Rojas, R., Flörke, M., Wimmer, F., and Bianchi, A.: Ensemble projections of future streamflow droughts in Europe, *Hydrol. Earth Syst. Sci.*, 18, 85–108, doi: 10.5194/hess-18-85-2014, 2014.
- 645 Fundel, F., Jörg-Hess, S., and Zappa, M.: Monthly hydrometeorological ensemble prediction of streamflow droughts and corresponding drought indices, *Hydrol. Earth Syst. Sci.*, 17, 395–407, doi:10.5194/hess-17-395-2013, 2013.
- Gu, L., Chen, J., Yin, J., Sullivan, S. C., Wang, H-M., Guo, S., Zhang, L., and Kim, J-S.: Projected increases in magnitude and socioeconomic exposure of global droughts in 1.5 and 2°C warmer climates, *Hydrol. Earth Syst. Sci.*, 24, 451–472, [https://doi.org/10.5194/hess-24-451-](https://doi.org/10.5194/hess-24-451-2020)
- 650 2020, 2020.
- Haile, G. G., Tang, Q., Sun, S., Huang, Z., Zhang, X., and Liu, X.: Droughts in East Africa: Causes, impacts and resilience, *Earth-Science Reviews*, 193, 146–161, <https://doi.org/10.1016/j.earscirev.2019.04.015>, 2019.
- Hannaford, J., Lloyd-Hughes, B., Keef, C., Parry, S., and Prudhomme, C.: Examining the large-scale spatial coherence of European drought using regional indicators of precipitation and streamflow deficit, *Hydrol. Process.*, 25, 1146–1162, doi:10.1002/hyp.7725, 2011.
- 655 Heudorfer, B., and Stahl, K.: Comparison of different threshold level methods for drought propagation analysis in Germany, *Hydrology Research*, 48.5, 1311–1326, doi:10.2166/nh.2016.258, 2017.
- Hisdal, H., Tallaksen, L. M., Clausen, B., Peters, E., and Gustard, A.: Hydrological Drought Characteristics. In: Tallaksen, L. M. & Van Lanen, H. A. J. (Eds.) *Hydrological Drought, Processes and Estimation Methods for Streamflow and Groundwater*. Development in Water Science 48, Elsevier Science B.V., pg. 139–198, 2004.
- 660 Ionita, M., Tallaksen, L. M., Kingston, D> G., Stagge, J. H., Laaha, G., Van Lanen, H. A. J., Scholz, P., Chelcea, S. M., and Haslinger, K.: The european 2015 drought from a climatological perspective, *Hydrol. Earth Syst. Sci.*, 21, 1397–1419, doi:10.5194/hess-21-1397-2017, 2017.
- IPCC.: *Climate Change 2014: Synthesis Report*. Contribution of Working Groups I, II and III to the Fifth Assessment Report of the Intergovernmental Panel on Climate Change [Core Writing Team, R.K. Pachauri and L.A. Meyer (eds.)]. IPCC, Geneva, Switzerland, 151 pp,
- 665 2014.
- Jakubowski, W., and Radczuk, L.: *Estimation of Hydrological Drought Characteristics, NIZOWKA2003 – Software Manual*, on accompanying CD to: *Hydrological Drought – Processes and Estimation Methods for Streamflow and Groundwater*, edited by: Tallaksen, L. M. and van Lanen, H. A. J., *Developments in Water Science*, 48, Elsevier Science B.V., Amsterdam, 2004.
- Laaha, G., Gauster, T., Tallaksen, L. M., Vidal, J-P., Stahl, K., Prudhomme, C., Heudorfer, B., Vlnas, R., Ionita, M., Van Lanen, H. A. J.,
- 670 Adler, M-J., Cailouet, L., Delus, C., Fendekova, M., Gailliez, S., Hannaford, J., Kingston, D., Van Loon, A. F., Mediero, L., Ozuch, M., Romanowicz, R., Sauquet, E., Stagge, J. H., and Wong, W. K.: The european 2015 drought from a hydrological perspective, *Hydrol. Earth Syst. Sci.*, 21, 3001–3024, doi:10.5194/hess-21-3001-2017, 2017.

- March, H., Domènech, L., and Saurí, D.: Water conservation campaigns and citizen perceptions: the drought of 2007-2008 in the Metropolitan area of Barcelona, *Nat. Hazards*, 65, 1951-1966, doi:10.1007/s11069-012-0456-2, 2013.
- 675 Martin-Ortega, J., González-Eguino, M., and Markandya, A.: The costs of drought: the 2007/2008 case of Barcelona, *Water Policy*, 14, 539-560, doi:10.2166/wp.2011.121, 2012.
- Marx, A., Kumar, R., Thober, S., Rakovec, O., Wanders, N., Zink, M., Wood, E. F., Pan, M., Sheffield, J., and Samaniego, L.: Climate change alters low flows in Europe under global warming of 1.5, 2, and 3°C, *Hydrol. Earth Syst. Sci.*, 22, 1017–1032, doi:10.5194/hess-22-1017-2018, 2018.
- 680 McKee, T. B., Doesken, N. J., and Kleist, J.: The relationship of drought frequency and duration to time scales. In: *Proceedings of the 8th Conference on Applied Climatology*, Vol. 17, American Meteorological Society Boston, MA, pp. 179–183, 1993.
- Mendoza, P. A., Wood, A. W., Clark, E., Rothwell, E., Clark, M. P., Nijssen, B., Brekke, L. D., and Arnold, J. R.: An intercomparison of approaches for improving operational seasonal streamflow forecasts, *Hydrol. Earth Syst. Sci.*, 21, 3915–3935, doi:10.5194/hess-21-3915-2017, 2017.
- 685 Mishra, A. K., and Singh, V. P.: A review of drought concepts, *Journal of Hydrology*, 391, 202-216, <https://doi.org/10.1016/j.jhydrol.2010.07.012>, 2010.
- Mishra, A.K., and Desai, V.R.: Drought forecasting using stochastic models, *Stoch. Environ. Res. Ris. Assess.*, 19, 326–339, <https://doi.org/10.1007/s00477-005-0238-4>, 2005.
- Nalbantis, I., and Tsakiris, G.: Assessment of hydrological drought revisited, *Water Resour. Manage.*, 23, 881-897, doi:10.1007/s11269-008-690 9305-1, 2009.
- Pappenberger, F., Thielen, J., and Del Medico, M.: The impact of weather forecast improvements on large scale hydrology: analyzing a decade of forecasts of the European Flood Alert System, *Hydrol. Process.*, 25, 1091–1113, <https://doi.org/10.1002/hyp.7772>, 2011.
- Pechlivanidis, I. G., Crochemore, L., Rosberg, J., and Bosshard, T.: What are the key drivers controlling the quality of seasonal streamflow forecasts? *Water Resources Research*, 56, e2019WR026987, <https://doi.org/10.1029/2019WR026987>, 2020.
- 695 Peel, M. C., Finlayson, B. L., and McMahon, T. A.: Updated world map of the Köppen-Geiger climate classification, *Hydrol. Earth Syst. Sci.*, 11, 1633–1644, 2007.
- Peters, E., Bier, G., Van Lanen, H. A. J., and Torfs, P. J. J. F.: Propagation and spatial distribution of drought in a groundwater catchment, *J. Hydrol.*, 321, 257–275, doi:10.1016/j.jhydrol.2005.08.004, 2006.
- Peters, E. P., Torfs, J. J. F., Van Lanen, H. A. J., and Bier, G.: Propagation of drought through groundwater-a new approach using linear 700 reservoir theory, *Hydrol. Process.*, 17, 3023-3040, 2003.
- Pfister, C., Weingartner, R., and Luterbacher, J.: Hydrological winter droughts over the last 450 years in the upper Rhine basin: a methodological approach, *Hydrological Sciences Journal*, 51:5, 966-985, doi:10.1623/hysj.51.5.966, 2006.
- Poljanšek, K., Marin Ferrer, M., De Groeve, T., and Clark, I.: Science for disaster risk management 2017: knowing better and losing less, executive summary, EUR 28034 EN, ISBN 978-92-79-60679-3, <https://doi.org/10.2788/842809>, JRC102482, 2017.
- 705 Pozzi, W., Sheffield, J., Stefanski, R., Cripe, D., Pulwarty, R., Vogt, J. V., Heim Jr, R. R., Brewer, M. J., Svoboda, M., Westerhoff, R.,, and Lawford, R.: Toward global drought early warning capability: Expanding international cooperation for the development of a framework for monitoring and forecasting, *Bulletin of the American Meteorological Society*, 94 (6), 776–785, <https://doi.org/10.1175/BAMS-D-11-00176.1>, 2013.
- Prudhomme, C., Giuntoli, I., Robinson, E. L., Clark, D. B., Arnell, N. W., Dankers, R., Fekete, B. M., Fransses, W., Gerten, D., Gosling, 710 S. N., Hagemann, S., Hannah, D. M., Kim, H., Masaki, Y., Satoh, Y., Stacke, T., Wada, Y., and Wisser, D.: Hydrological droughts

- in the 21st century, hotspots and uncertainties from a global multimodel ensemble experiment, *PNAS*, vol.111, no.9, 3262-3267, doi:10.1073/pnas.1222473110, 2014.
- Prudhomme, C., Parry, S., Hannaford, J., Clark, D. B., Hageman, S., and Voss, F.: How well do large-scale models reproduce regional hydrological extremes in Europe? *Journal of Hydrometeorology*, 12, 1181-1204, doi:10.1175/2011JHM1387.1, 2011.
- 715 Samaniego, L., Thober, S., Kumar, R., Wanders, N., Rakovec, O., Pan, M., Zink, M., Sheffield, J., Wood, E. F., and Marx, A.: Anthropogenic warming exacerbates European soil moisture droughts, *Nature Climate Change*, 8, 421-426, doi:10.1038/s41558-018-0138-5, 2018.
- Sarailidis, G., Vasiliades, L., and Loukas, A.: Analysis of streamflow droughts using fixed and variable thresholds, *Hydrological Processes*, 33, 414-431, <https://doi.org/10.1002/hyp.13336>, 2019.
- Schaake, J. C., Hamill, T. M., Buizza, R., and Clark, M.: HEPEX: the hydrological ensemble prediction experiment, *Bulletin of the American Meteorological Society*, 88(10), 1541-1547, 2007.
- 720 Sepulcre-Canto, G., Horion, S., Singleton, A., Carrao, H., and Vogt, J.: Development of a combined drought indicator to detect agricultural drought in Europe, *Nat. Hazards Earth Syst. Sci.*, 12, 3519-3531, <https://doi.org/10.5194/nhess-12-3519-2012>, 2012.
- Sivakumar, M. V. K., Stefanski, R., Bazza, M., Zelaya, S., Wilhite, D., and Magalhaes, A. R.: High Level Meeting on National Drought Policy: Summary and Major Outcomes, *Weather and Climate Extremes*, 3, 126-132, <http://dx.doi.org/10.1016/j.wace.2014.03.007>, 2014.
- 725 Slater, L.J., and Villarini, G.: Enhancing the predictability of seasonal streamflow with a statistical-dynamical approach, *Geophysical Research Letters*, 45(13), pp.6504-6513, 2018.
- Stahl, K., Kohn, I., Blauhut, V., Urquijo, J., De Stefano, L., Aca'cio, V., Dias, S., Stagge, J. H., Tallaksen, L. M., Kampragou, E., . . . , and Van Lanen, H. A. J.: Impacts of european drought events: insights from an international database of text-based reports., *Natural Hazards and Earth System Sciences*, 16 (3), 801-819, <https://doi.org/10.5194/nhess-16-801-2016>, 2016.
- 730 Stockdale, T., Johnson, S., Ferranti, L., Balmaseda, M., and Briceag, S.: ECMWF's new long range forecasting system SEAS5, Vol. 154. *ECMWF Newsletter*, doi:10.21957/tsb6n1, 2018.
- Sung, J. H., and Chung, E.-S.: Development of streamflow drought severity-duration-frequency curves using the threshold level method, *Hydrol. Earth Syst. Sci.*, 18, 3341-3351, doi:10.5194/hess-18-3341-2014, 2014.
- Sutanto, S. J., Van Lanen, H. A. J., Wetterhall, F., and Llorca, X.: Potential of pan-European seasonal hydro-meteorological drought forecasts obtained from a Multi-Hazard Early Warning System, *Bulletin of the American Meteorological Society*, 101, 368-393, <https://doi.org/10.1175/BAMS-D-18-0196.1>, 2020a.
- 735 Sutanto, S. J., Wetterhall, F., and Van Lanen, H. A. J.: Hydrological drought forecasts outperform meteorological drought forecasts, *Environ. Res. Lett.*, 15, 084010, <https://doi.org/10.1088/1748-9326/ab8b13>, 2020b.
- Sutanto, S. J., and van Lanen, H. A. J.: Hydrological drought characteristics based on groundwater and runoff across Europe, *Proc. IAHS*, 740 383, 281-290, <https://doi.org/10.5194/piahs-383-281-2020>, 2020.
- Sutanto, S. J., Van der Weert, M., Wanders, N., Blauhut, V., and Van Lanen, H. A. J.: Moving from drought hazard to impact forecasts, *Nat. Comm.*, 10:495, <https://doi.org/10.1038/s41467-019-12840-z>, 2019.
- Tallaksen, L. M., Hisdal, H., and Van Lanen, H. A. J.: Space-time modeling of catchment scale drought characteristics, *Journal of Hydrology*, 375, 363-372, 2009.
- 745 Tallaksen, L. M., and Van Lanen, H. A. J.: Hydrological drought: processes and estimation methods for streamflow and groundwater, In: *Developments in Water Science*, vol. 48, Amsterdam, the Netherlands: Elsevier Science B.V, 2004.
- Tallaksen, L. M., Madsen, H., and Clausen, B.: On the definition and modeling of streamflow drought duration and deficit volume, *Hydrological Sciences Journal*, 42:1, 15-33, doi:10.1080/02626669709492003, 1997.

- Thielen, J., Bartholmes, J., Ramos, M.-H., and Roo, A. D.: The European Flood Alert System - part 1: concept and development, *Hydrol. Earth Syst. Sci.*, 13, 125–140, <https://doi.org/10.5194/hess-13-125-2009>, 2009.
- Tijdeman, E., Stahl, K., and Tallaksen, L. M.: Drought characteristics derived based on the Standardized Streamflow Index: A large sample comparison for parametric and nonparametric methods, *Water Resources Research*, 56, e2019WR026315, <https://doi.org/10.1029/2019WR026315>, 2020.
- Trambauer, P., Werner, M., Winsemius, H. C., Maskey, S., Dutra, E., and Uhlenbrook, S.: Hydrological drought forecasting and skill assessment for the Limpopo River basin, southern Africa, *Hydrology and Earth System Sciences*, 19(4), 1695–1711, 2015.
- Trambauer, P., Maskey, S., Winsemius, H., Werner, M., and Uhlenbrook, S.: A review of continental scale hydrological models and their suitability for drought forecasting in (sub-Saharan) Africa, *Physics and Chemistry of the Earth*, 66, 16–26, 2013.
- Van Der Knijff, J. M., Younis, J., and De Roo, A. P. J.: Lisflood: a gis-based distributed model for river basin scale water balance and flood simulation, *International Journal of Geographical Information Science*, 24:2, 189–212, <https://doi.org/10.1080/13658810802549154>, 2010.
- Van Der Knijff, J.: LISVAP: Evaporation Pre-Processor for the LISFLOOD Water Balance and Flood Simulation Model, EUR 22639 EN/2, 2008.
- Van Dijk, A. I. J. M., Beck, H. E., Crosbie, R. S., de Jeu, R. A. M., Liu, Y. Y., Podger, G. M., Timbal, B., and Viney, N. R.: The Millennium Drought in southeast Australia (2001–2009): Natural and human causes and implications for water resources, ecosystems, economy, and society, *Water Resources Research*, 49, 1040–1057, doi:10.1002/wrcr.20123, 2013.
- Van Hateren, T., Sutanto, S. J., and Van Lanen, H. A. J.: Evaluating uncertainty and robustness of seasonal meteorological and hydrological drought forecasts at the catchment scale-case Catalonia (spain), *Env. Int.*, 133, 105206, <https://doi.org/10.1016/j.envint.2019.105206>, 2019.
- Van Lanen, H. A. J., Wanders, N., Tallaksen, L. M., and Van Loon, A. F.: Hydrological drought across the world: impact of climate and physical catchment structure, *Hydrol. Earth Syst. Sci.*, 17, 1715–1732, doi:10.5194/hess-17-1715-2013, 2013.
- Van Lanen, H. A. J., Fendeková, M., Kupczyk, E., Kasprzyk, A., and Pokojski, W.: Flow Generating Processes, in: *Hydrological Drought, Processes and Estimation Methods for Streamflow and Groundwater*, edited by: Tallaksen, L. M. and Van Lanen, H. A. J., Development in Water Science 48, Elsevier Science B.V., 53–96, 2004.
- Van Loon, A. F., Rangelcroft, S., Coxon, G., Naranjo, J. A. B., Ogtrop, F. V., and Van Lanen, H. A. J.: Using paired catchments to quantify the human influence on hydrological droughts, *Hydrol. Earth Syst. Sci.*, 23, 1725–1739, <https://doi.org/10.5194/hess-23-1725-2019>, 2019.
- Van Loon, A. F.: Hydrological drought explained, *WIREs Water*, <https://doi.org/10.1002/wat2.1085>, 2015.
- Van Loon, A. F., and Van Lanen, H. A. J.: A process-based typology of hydrological drought, *Hydrol. Earth Syst. Sci.*, 16, 1915–1946, 2012.
- Van Loon, A. F., Van Huijgevoort, M. H. J., and Van Lanen, H. A. J.: Evaluation of drought propagation in an ensemble mean of large-scale hydrological models, *Hydrol. Earth Syst. Sci.*, 16, 4057–4078, doi:10.5194/hess-16-4057-2012, 2012.
- Van Loon, A. F., Fendeková, M., Hisdal, H., Horvát, O., Van Lanen, H. A. J., Machlica, A., Oosterwijk, J., and Tallaksen, L. M.: Understanding hydrological winter drought in Europe, in: 6th World FRIEND Conference “Global Change: Facing Risks and Threats to Water Resources”, edited by: Servat, E., Demuth, S., Dezetter, A., Daniell, T., Ferrari, E., Ijjaali, M., Jabrane, R., Van Lanen, H. A. J., and Huang, Y., IAHS-AISH P., 340, 189–197, 2010.
- Vicente-Serrano, S. M., López-Moreno, J. I., Beguería, S., Lorenzo-Lacruz, J., Azorin-Molina, C., and Morán-Tejeda, E.: Accurate computation of a streamflow drought index, *J. Hydrol. Eng.*, 17(2), 318–332, doi:10.1061/(ASCE)HE.1943-5584.0000433, 2012.

- Vicente-Serrano, S. M., Begueria, S., and López-Moreno, J. I.: A multi-scalar drought index sensitive to global warming: the standardized precipitation evapotranspiration index-SPEI, *Journal of Climate*, 23(7), 1696–1718, <https://doi.org/10.1175/2009JCLI2909.1>, 2010.
- Vidal, J.-P., Martin, E., Franchistéguy, L., Habets, F., Soubeyroux, J.-M., Blanchard, M., and Baillon, M.: Multilevel and multiscale drought reanalysis over France with the Safran-Isba-Modcou hydrometeorological suite, *Hydrol. Earth Syst. Sci.*, 14, 459–478, <https://doi.org/10.5194/hess-14-459-2010>, 2010.
- 790 Vogel, R. M., and Stedinger, J. R.: Generalized storage-reliability-yield relationships, *J. Hydrol.*, 89, 303-327, 1987.
- Wanders, N., Wada, Y., and Van Lanen, H. A. J.: Global hydrological droughts in the 21st century under a changing hydrological regime, *Earth Syst. Dynam.*, 6, 1-15, 2015.
- Wanders, N., Thober, S., Kumar, R., Pan, M., Sheffield, J., Samaniego, L., and Wood, E.: Development and evaluation of a Pan-European multi-model seasonal hydrological forecasting system, *Journal of Hydrometeorology*, 20, 99-115, 2019.
- 795 Wilhite, D. A., Svoboda, M. D., and Hayes, M. J.: Understanding the complex impacts of drought: A key to enhancing drought mitigation and preparedness, *Water Resour. Manage.*, 21, 763–774, doi:10.1007/s11269-006-9076-5, 2007.
- WMO & GWP.: National Drought Management Policy Guidelines: A Template for Action (D. A. Wilhite). Integrated Drought Management Programme (IDMP) Tools and Guidelines Series 1. WMO, Geneva, Switzerland and GWP, Stockholm, Sweden, [\[https://public.wmo.int/en/resources/library/national-drought-management-policy-guidelines-template-action\]](https://public.wmo.int/en/resources/library/national-drought-management-policy-guidelines-template-action), 2014.
- 800 Wong, W. K., Beldring, S., Engen-Skaugen, T., Haddeland, I., and Hisdal, H.: Climate Change Effects on Spatiotemporal Patterns of Hydro-climatological Summer Droughts in Norway, *J. Hydrometeorol.*, 12, 1205–1220, doi:10.1175/2011JHM1357.1, 2011.
- Yevjevich, V.: An objective approach to definition and investigations of continental hydrologic droughts, *Hydrology Papers*, 23, Colorado State University, Fort Collins, USA, 1967.
- 805 Yuan X., Zhang, M., Wang, L., and Zhou, T.: Understanding and seasonal forecasting of hydrological drought in the Anthropocene, *Hydrol. Earth Syst. Sci.*, 21, 5477–5492, doi:10.5194/hess-21-5477-2017, 2017.

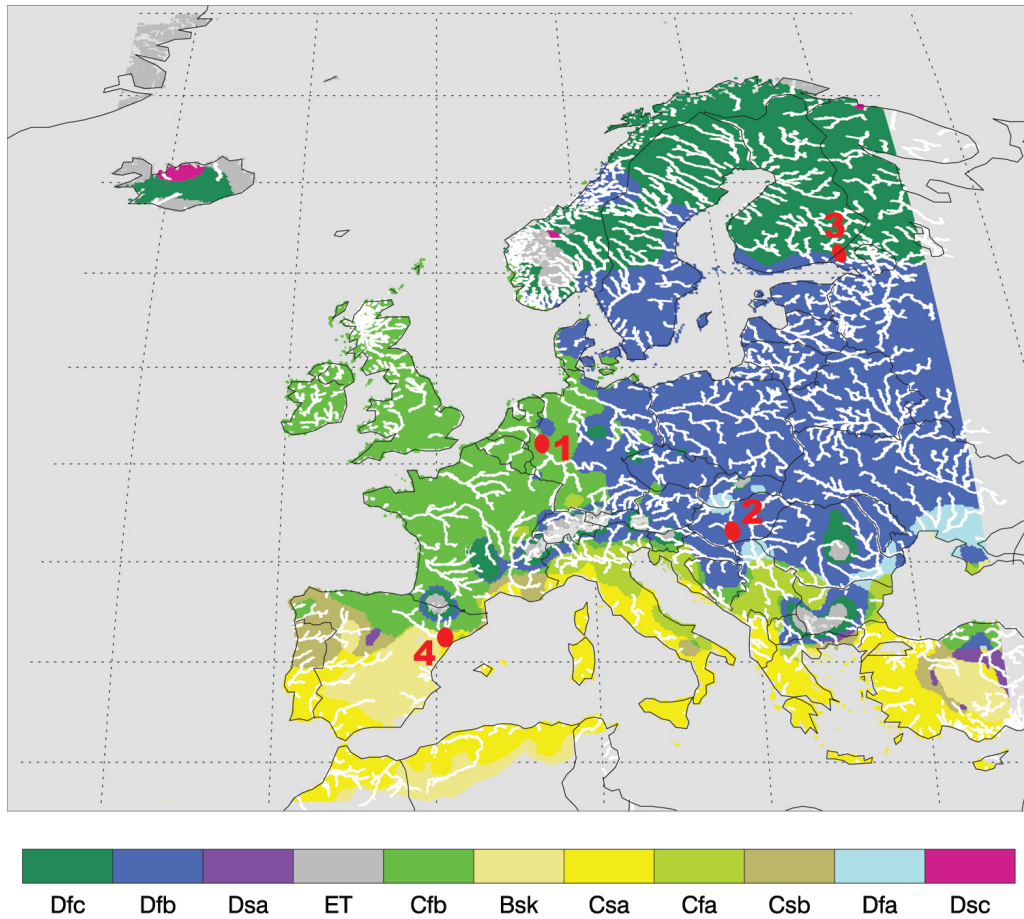


Figure 1. Köppen-Geiger map of Europe and locations of selected river basins for detailed hydrological drought analyses in different climate regimes, as shown by red dots. Readers are referred to Peel et al. (2007) for an explanation of Köppen-Geiger climate classification codes (e.g., Dfc, Dfb, Cfb, and so on).

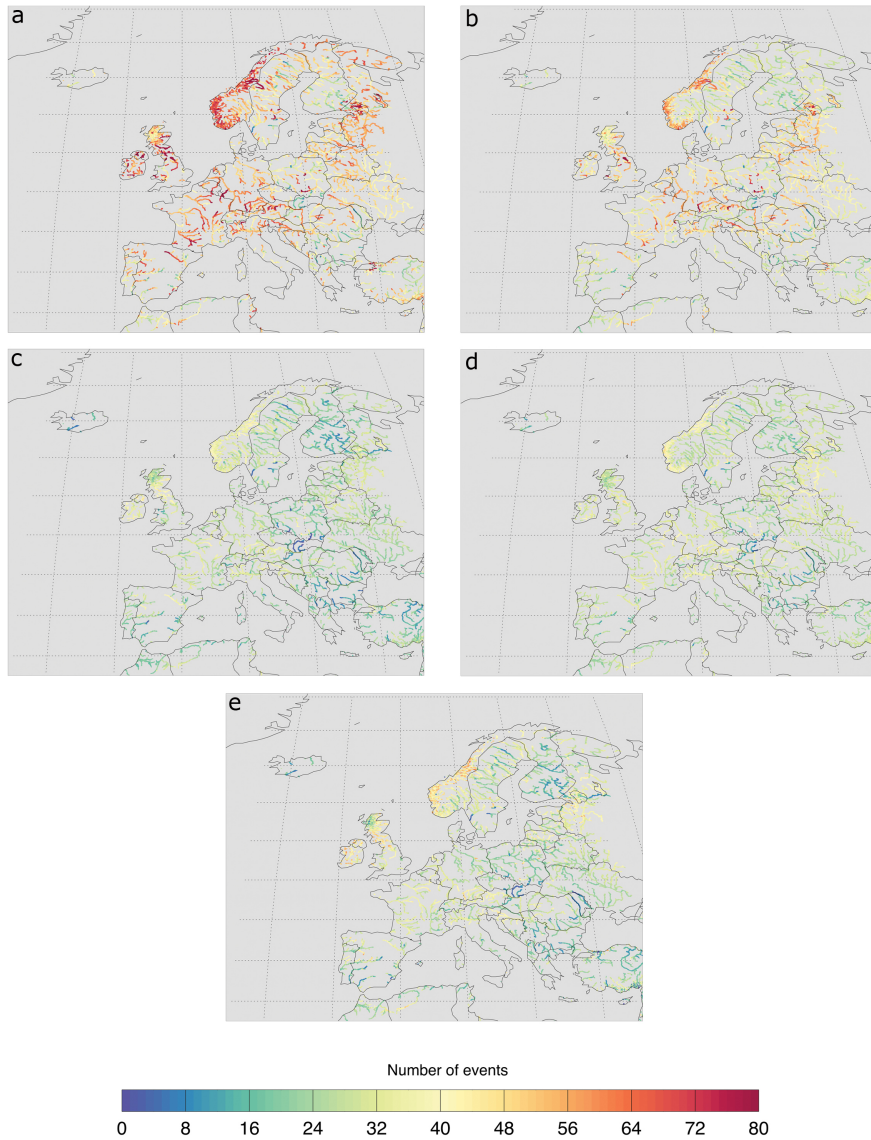


Figure 2. Drought occurrences in European rivers from October 1990 to September 2018 (28 years) identified using different drought identification methods: a) the variable threshold method with daily streamflow data (VTD drought), b) the fixed threshold method with daily streamflow data (FTD drought), c) the variable threshold method with monthly streamflow data (VTM drought), d) the fixed threshold method with monthly streamflow data (FTM drought), and e) the Standardized Streamflow Index with accumulation time 1 month (SSI-1 drought).

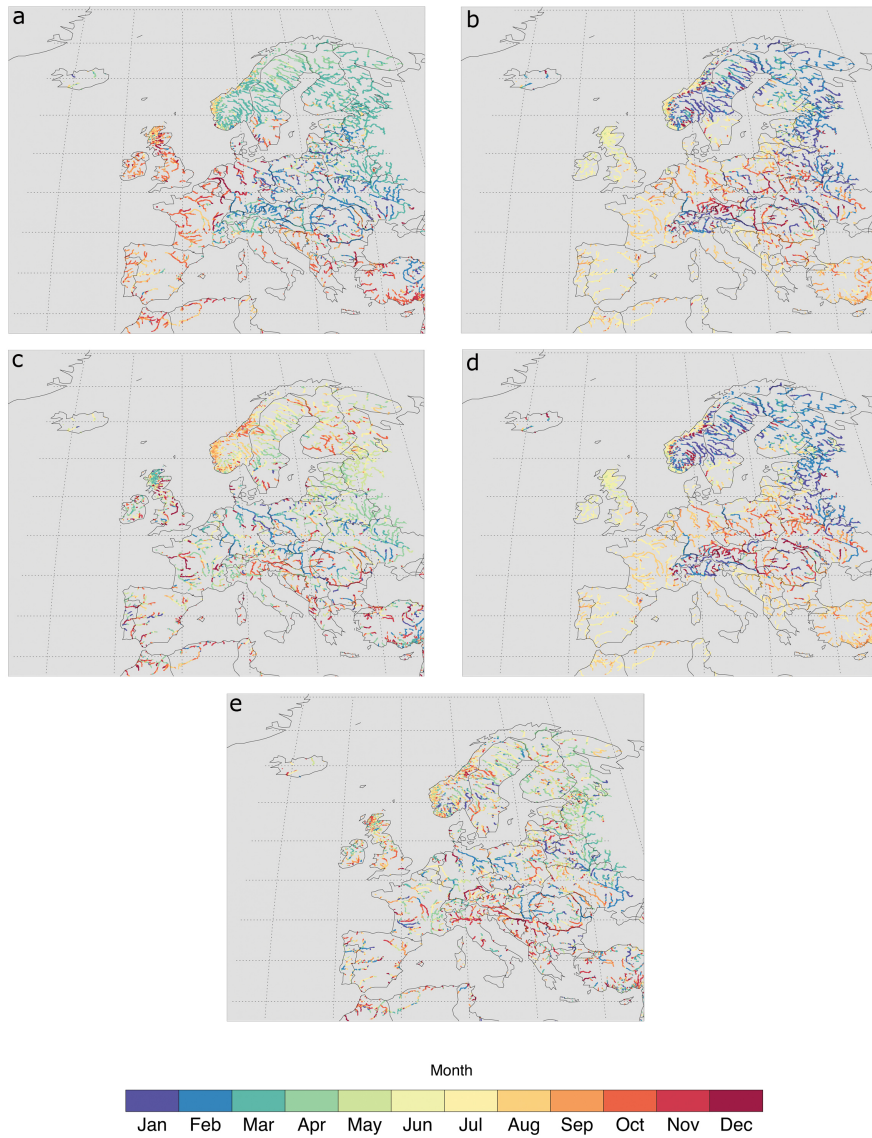


Figure 3. Months when drought mostly started in the European rivers from October 1990 to September 2018 identified using different drought identification methods: a) the VTD drought, b) the FTD drought, c) the VTM drought, d) the FTM drought, and e) the SSI-1 drought. For an explanation of the acronyms, see Fig. 2.

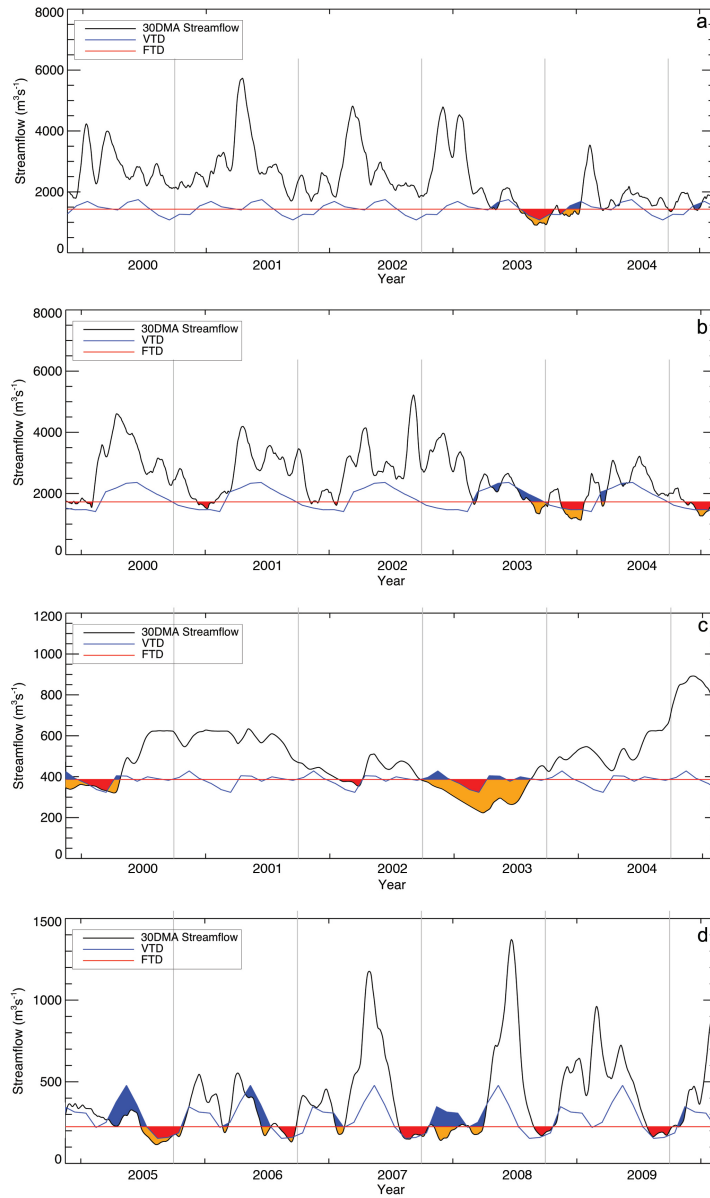


Figure 4. Streamflow droughts analyzed using daily streamflow data and different drought identification methods for the: a) Rhine River from 2000 to 2004 (location 1), b) Danube River from 2000 to 2004 (location 2), c) Vuoksi River from 2000 to 2004 (location 3), and d) Ebro River from 2005 to 2009 (location 4). Streamflow drought events are indicated as blue areas below the threshold for the VTD drought and red areas for the FTD drought. Orange areas indicate both VTD and FTD drought occurrences. Light grey lines show the start of hydrologic years (October). Locations are specified in Fig. 1.

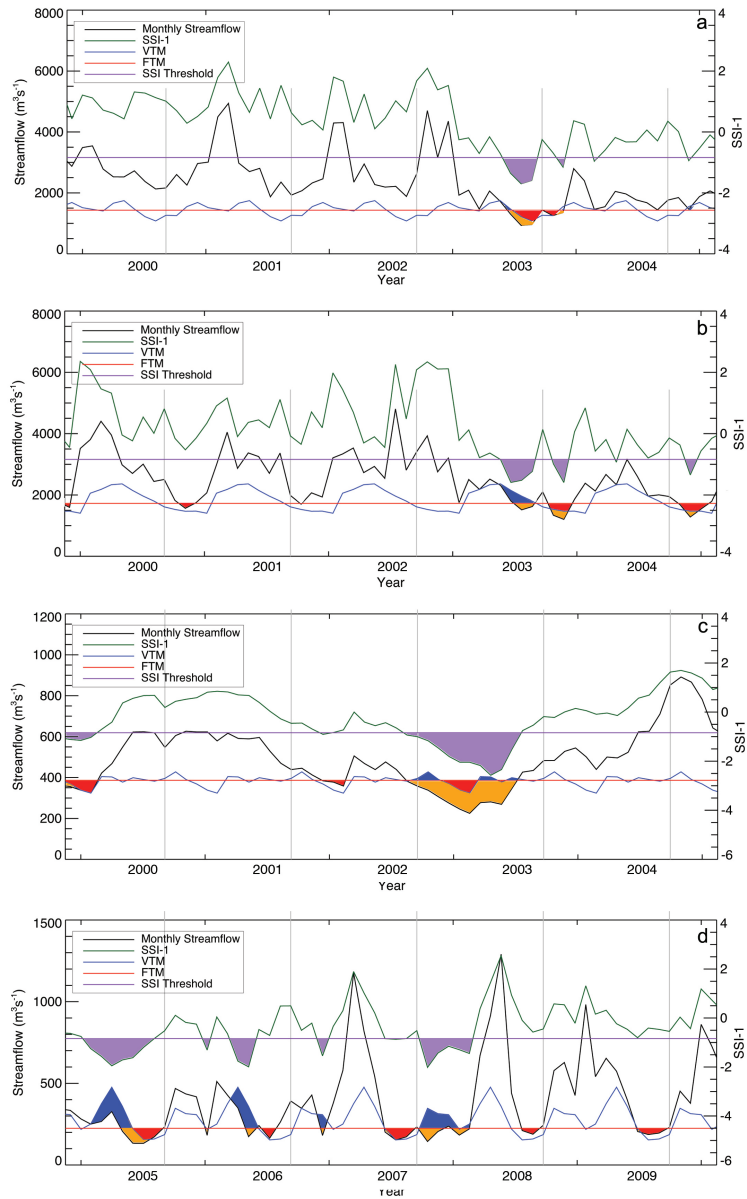


Figure 5. Streamflow droughts analyzed using monthly streamflow data derived from daily streamflow and different drought identification methods for the: a) Rhine River from 2000 to 2004 (location 1), b) Danube River from 2000 to 2004 (location 2), c) Vuoksi River from 2000 to 2004 (location 3), and d) Ebro River from 2005 to 2009 (location 4). Streamflow drought events are indicated as blue areas below the VTM drought, red areas for the FTM drought, and purple areas for the SSI-1 drought. Orange areas indicate both VTM and FTM drought occurrences. Light grey lines show the start of hydrologic years (October). Locations are specified in Fig. 1.

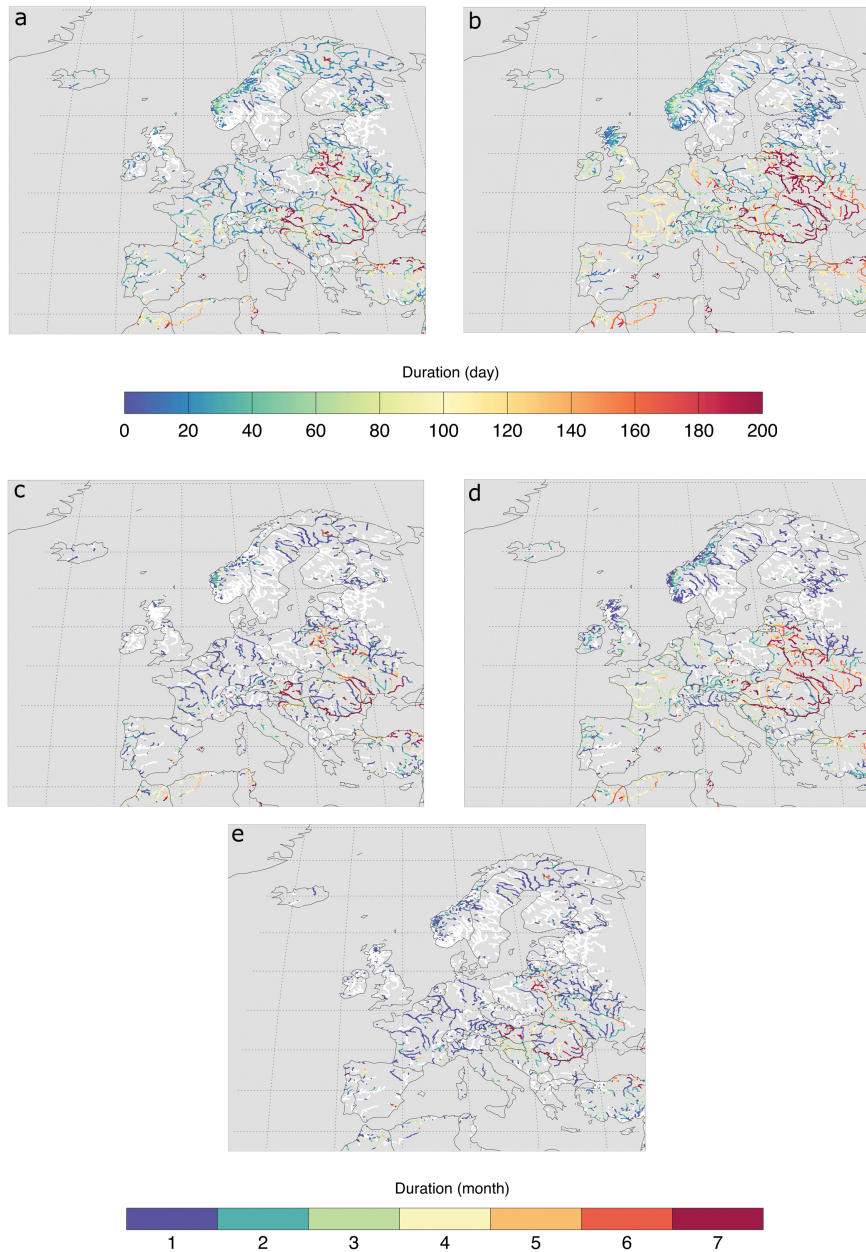


Figure 6. Forecasted average duration of drought events (median of 25 ensemble members) in the European rivers using different drought identification methods and the forecast initiated on 1st July 2003 with a lead time 7-month for: a) the VTD drought, b) the FTD drought, c) the VTM drought, d) the FTM drought, and e) the SSI-1 drought. White river color indicates that no drought was forecasted.

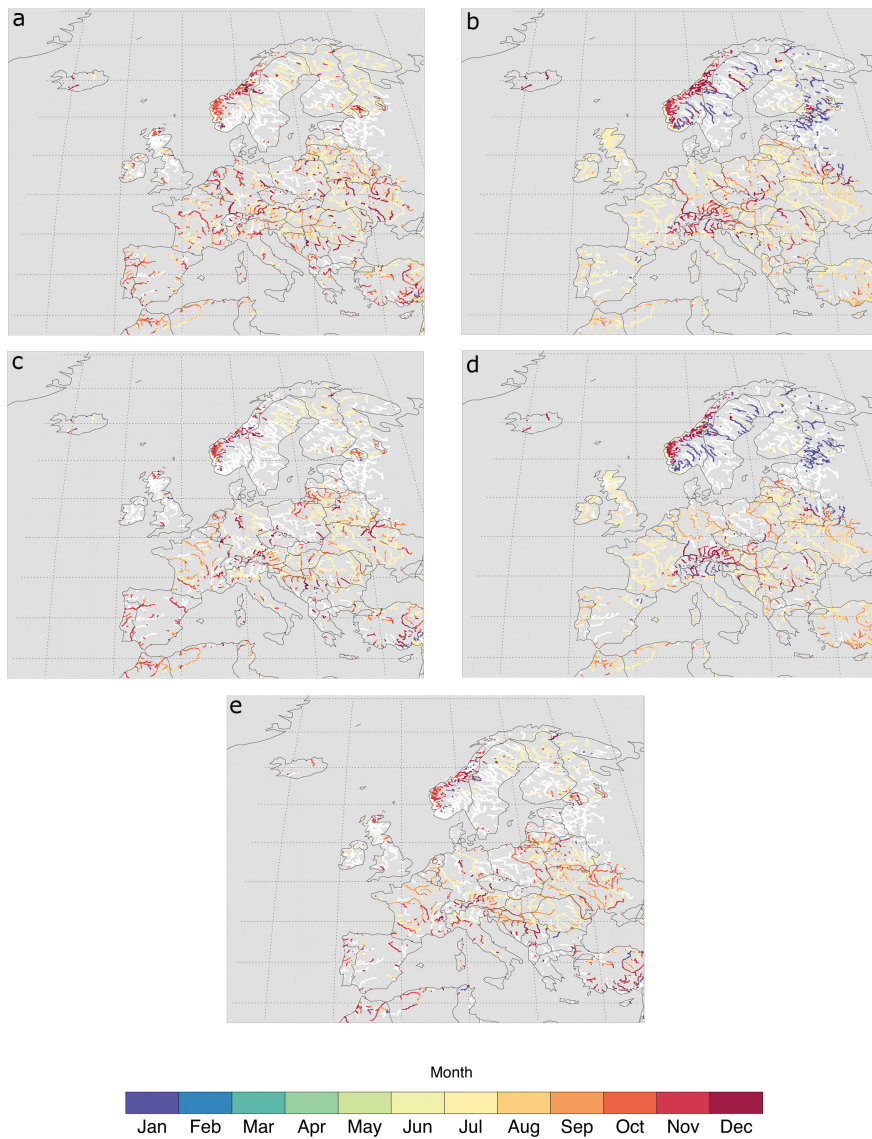


Figure 7. Months when drought is forecasted to start in the European rivers using different drought identification methods and the forecast initiated on 1st July 2003 with a lead time 7-month for: a) the VTD drought, b) the FTD drought, c) the VTM drought, d) the FTM drought, and e) the SSI-1 drought. White river color indicates that no drought was forecasted. Please note that in this case drought cannot start in Feb-June. Section 2.3 explains how the drought timing is determined using forecast data.

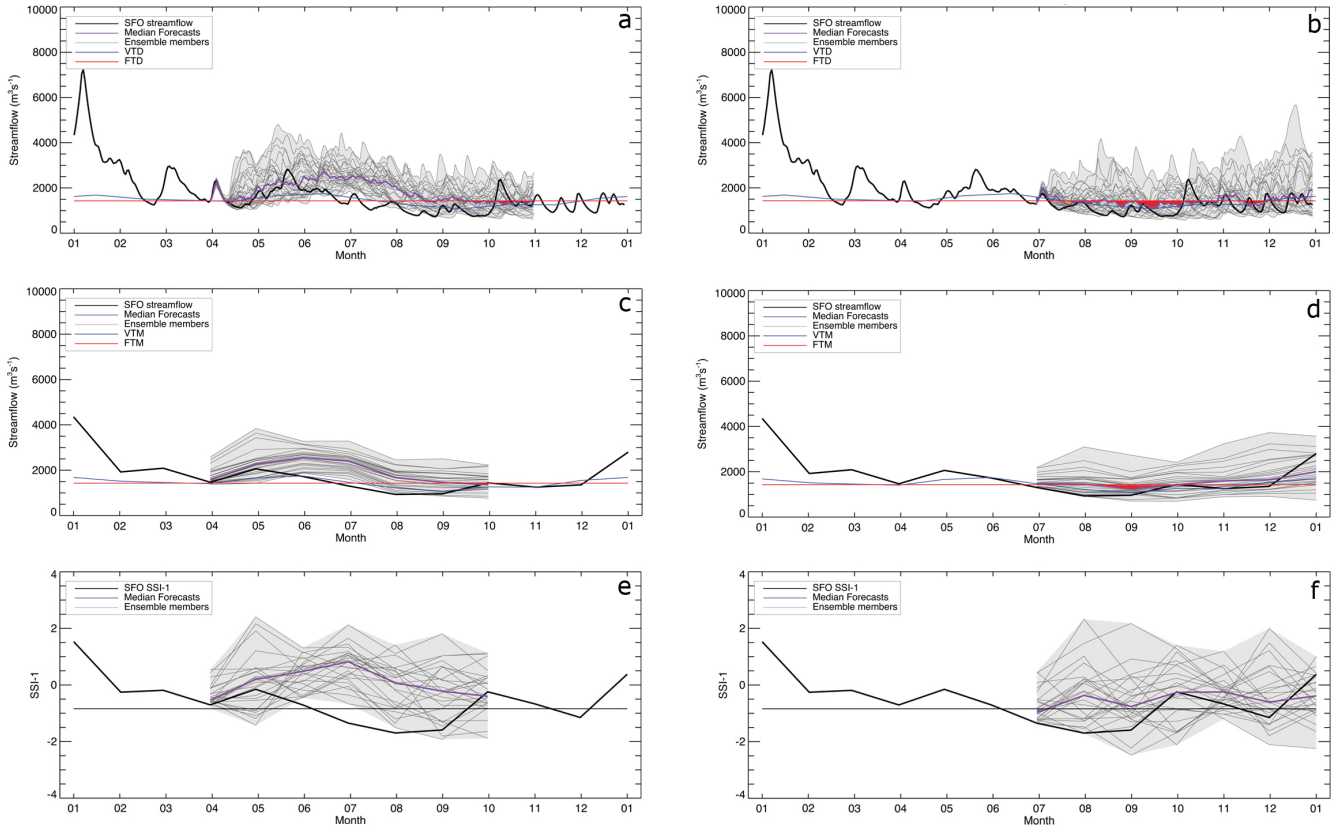


Figure 8. Observed (SFO) and forecasted streamflow (median and 25 ensemble members) of the Rhine River: a) daily streamflow drought (VTD and FTD) initiated on 1st April 2003 for 7 months ahead, c) monthly streamflow drought (VTM and FTM) initiated on 1st April 2003 for 7 months ahead, and e) forecasted SSI-1 drought initiated on 1st April 2003 for 7 months ahead. b), d), and f) same as a, c, and e, but for forecasts initiated on 1st July 2003. Droughts are indicated by blue shaded area for VTD and VTM, red shaded area for FTD and FTM, and purple shaded area for SSI-1. Orange areas indicate both VTD and FTD drought.

Table 1. Streamflow drought characteristics derived from daily streamflow data using the VTD and the FTD methods obtained from the hydrologic years 1991 to 2018 for the five climate regions in Europe and the entire Europe. N stands for number of events, T stands for timing (start month), D stands for duration (day), and DV stands for deficit volume (m³). D and DV are average drought characteristics and T is median drought timing for all river grid cells located in a climate region. Please note that Mediterranean region only consists of Bsk and Csa. Drought characteristics for Europe are obtained from the weighted average drought characteristics from each climate region considering the relative area in Europe (last column)

No	Region	Drought characteristics								Area % of Europe
		VTD				FTD				
		N	T	D	DV	N	T	D	DV	
1	ET	55.4	4	44	571	39.7	3	55.7	469	2.6
2	Dfb	48.3	3	43.8	1,113	42.4	6	51.9	1,197	40.6
3	Dfc	49.2	3	46.7	823	34.5	2	63.7	686	24
4	Cfb	57.8	10	36.4	886	45.1	7	47.2	901	14.9
5	Med	41	10	56.3	455	31.6	8	68.4	389	17.8
6	Europe	49.6	-	44.6	919	39.6	-	56	913	91.3

Table 2. Streamflow drought characteristics derived from monthly streamflow data using the VTM, the FTM, and the SSI-1 drought identification method obtained from the hydrologic years 1991 to 2018 for the five climate regions in Europe and the entire Europe. See Table 1 for drought characteristic abbreviations. The unit for drought duration is month

No	Region	Drought characteristics										
		VTM				FTM				SSI-1		
		N	T	D	DV	N	T	D	DV	N	T	D
1	ET	28.9	7	2.5	1,344	29.2	6	2.5	655	35.2	7	2.2
2	Dfb	26.5	5	2.5	1,727	29.1	7	2.5	1,619	29.5	5	2.2
3	Dfc	25.6	6	2.5	955	27.8	2	2.5	781	30	5	2.4
4	Cfb	30.7	5	1.9	1,495	30.4	7	2.2	1,314	34.8	7	1.9
5	Med	22.6	9	2.9	690	25.7	8	2.7	472	25.5	8	2.4
6	Europe	26.6	-	2.4	1,371	28.6	-	2.5	1,211	30.3	-	2.2

Table 3. Forecasted streamflow drought characteristics derived from daily streamflow data using the VTD and FTD approaches for the Rhine River initiated from 1st January 2003 to 1st December 2003 for 7 months ahead (215 days). Drought characteristics were derived using median of the ensemble. N stands for number of occurrence, Ne stands for maximum number of ensemble members falling below the drought threshold (%), T stands for timing (month), D stands for average duration (day), and DV stands for total deficit volume (m³)

Forecast initiation month	Drought characteristics									
	VTD					FTD				
	N	Ne	T	D	DV	N	Ne	T	D	DV
1	0	20	0	0	0	0	20	0	0	0
2	0	20	0	0	0	0	28	0	0	0
3	0	20	0	0	0	0	48	0	0	0
4	3	88	4	2.7	140	9	88	9	6.1	421
5	5	56	10	5	283	3	76	10	24	4,199
6	8	64	10	5.1	506	4	80	8	28.7	5,108
7	14	100	12	2.8	202	9	100	8	12.7	1,443
8	11	100	11	12.3	1,930	7	100	1	18	5,877
9	6	100	12	16.3	2,793	7	100	12	14.7	4,451
10	3	100	10	24	4,502	4	100	11	20.5	4,646
11	8	100	1	8.1	2,077	3	100	11	15.3	5,266
12	2	100	12	23	10,654	1	100	12	43	14,720

Table 4. Forecasted streamflow drought characteristics derived from monthly streamflow data using the VTM, the FTM, and the SSI-1 approaches for the Rhine River initiated from 1st January 2003 to 1st December 2003 for 7 months ahead (215 days). See Table 3 for drought characteristic abbreviations. The unit for average drought duration is month

Forecast initiation month	Drought characteristics													
	VTM					FTM					SSI-1			
	N	Ne	T	D	DV	N	Ne	T	D	DV	N	Ne	T	D
1	0	8	0	0	0	0	8	0	0	0	0	8	0	0
2	0	0	0	0	0	0	0	0	0	0	0	0	0	0
3	0	8	0	0	0	0	28	0	0	0	0	16	0	0
4	0	40	0	0	0	1	52	10	1	2,260	0	24	0	0
5	1	56	10	1	1,446	1	60	9	2	10,103	0	44	0	0
6	1	60	10	1	1,693	1	72	9	3	12,410	0	48	0	0
7	1	52	7	1	254	1	68	9	2	5,583	1	56	7	1
8	2	100	8	2	7,276	1	100	8	4	32,883	2	100	8	1.5
9	1	72	9	2	10,210	1	100	9	2	25,989	1	92	9	2
10	2	72	12	1	3,773	1	92	10	2	13,106	1	72	10	1
11	1	84	11	2	5,850	1	96	11	1	10,193	1	80	11	1
12	1	84	12	1	14,394	1	84	12	1	10,731	1	64	12	1

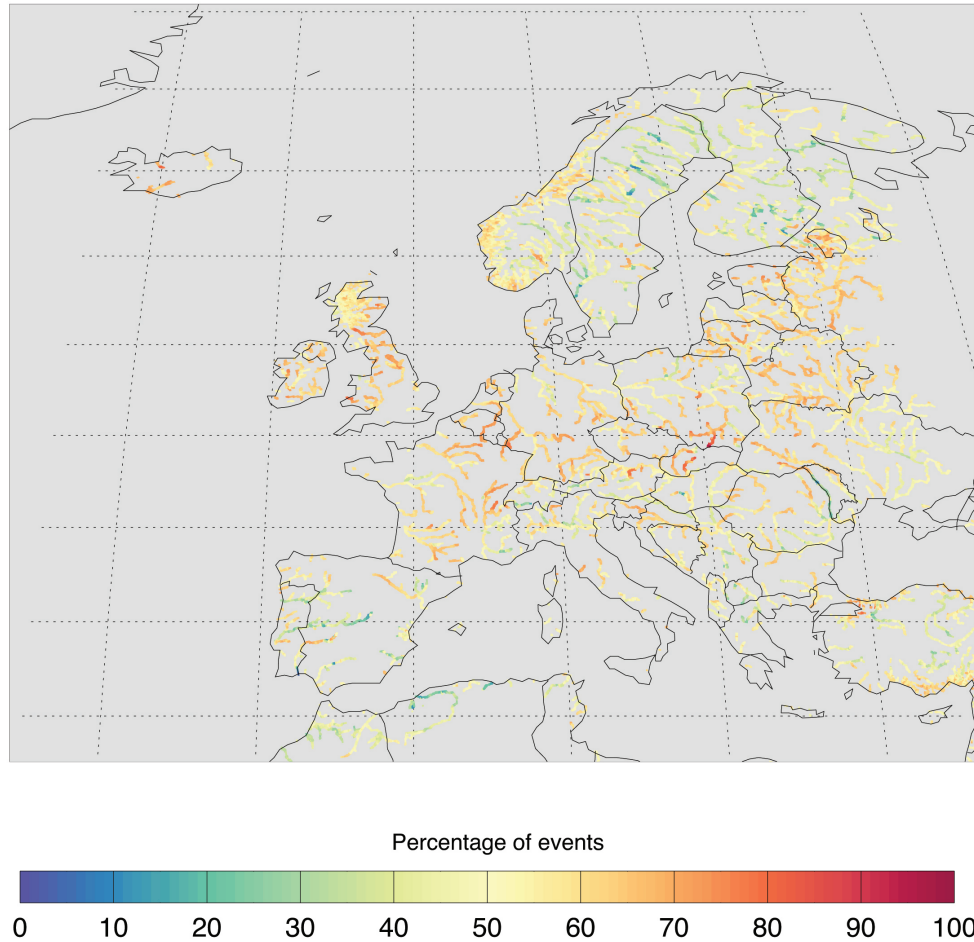


Figure A1. Minor drought occurrences (<30 days) in % of total number drought occurrences (Fig. 2) for the European rivers from October 1990 to September 2018 (28 years) identified using the variable threshold method with daily streamflow data (VTD drought).

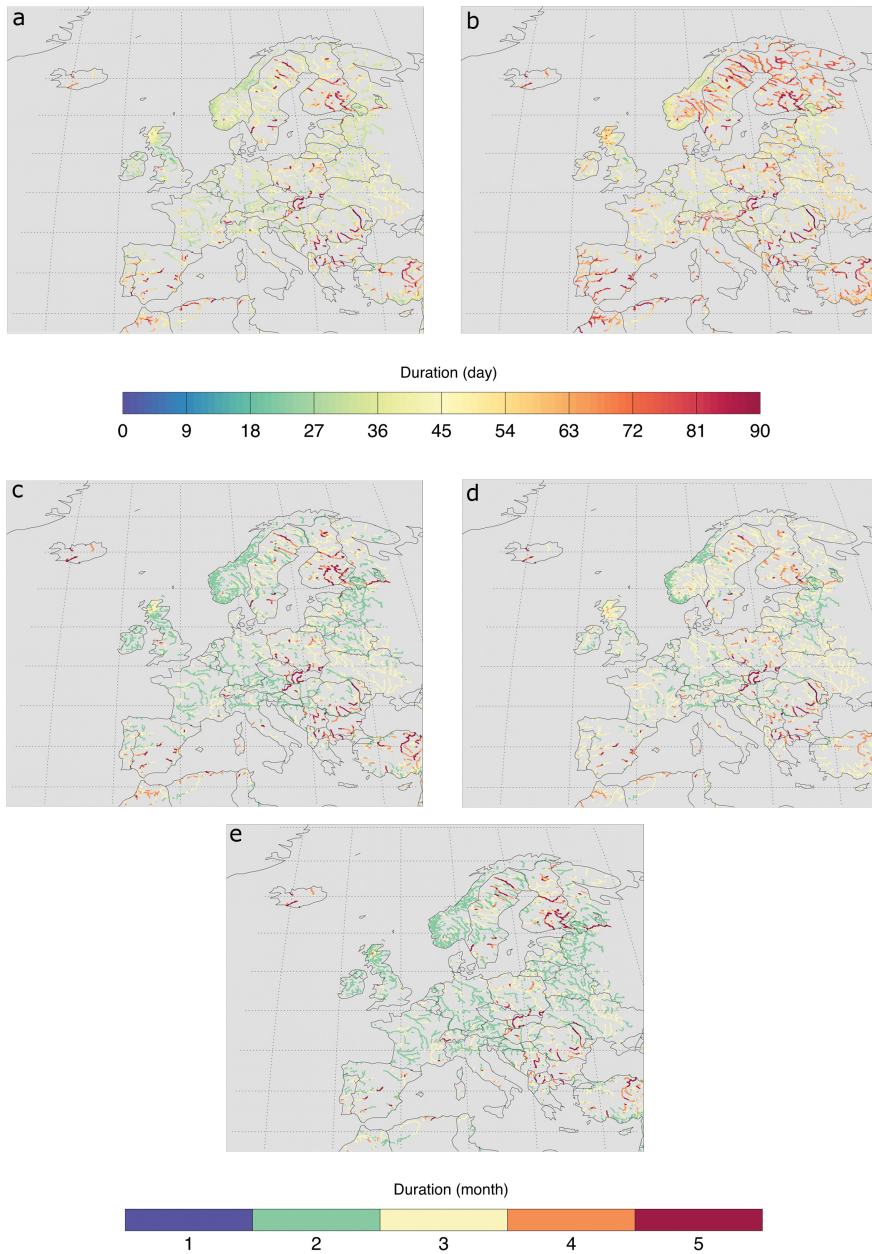


Figure A2. Average duration of drought events for the European rivers from October 1990 to September 2018 identified using different drought identification methods: a) the VTD, b) the FTD, c) the VTM, d) the FTM, and e) the SSI-1 approaches. For an explanation of the acronyms, see Fig. 2.

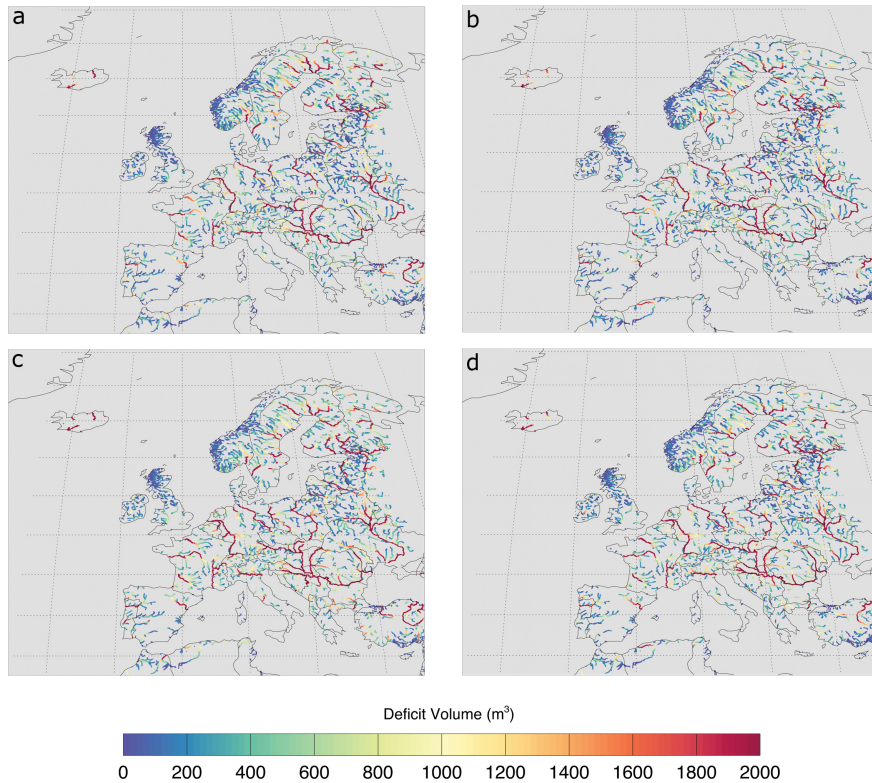


Figure A3. Average drought deficit volume for the European rivers from October 1990 to September 2018 identified using different drought identification methods: a) the VTD, b) the FTD, c) the VTM, and d) the FTM approaches. Note that deficit volume is not standardized.

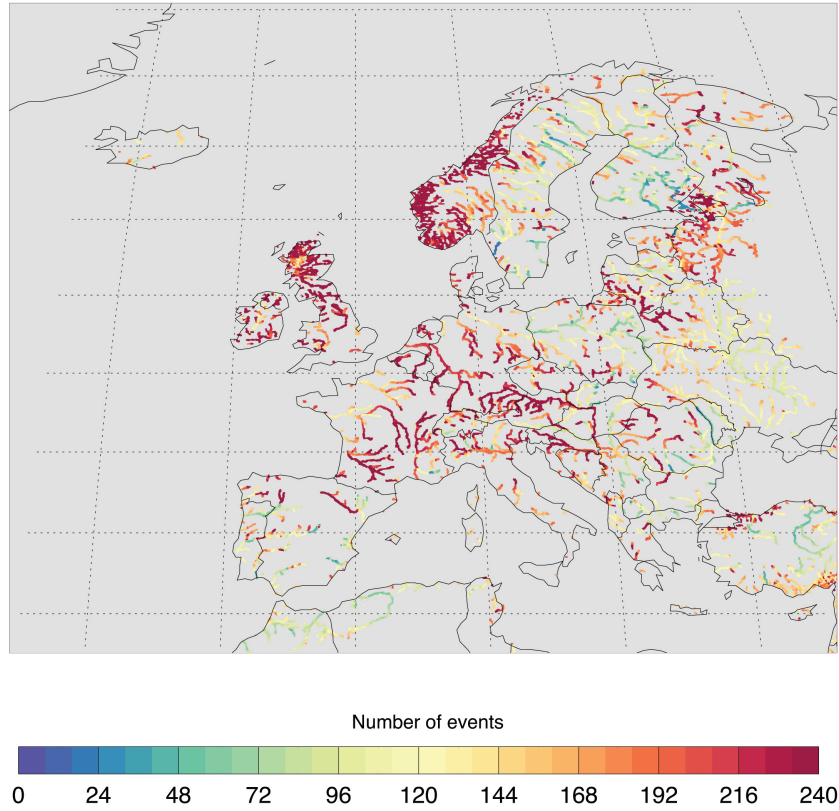


Figure A4. Drought occurrences in European rivers from October 1990 to September 2018 (28 years) identified using the VTD without the 30DMA application.

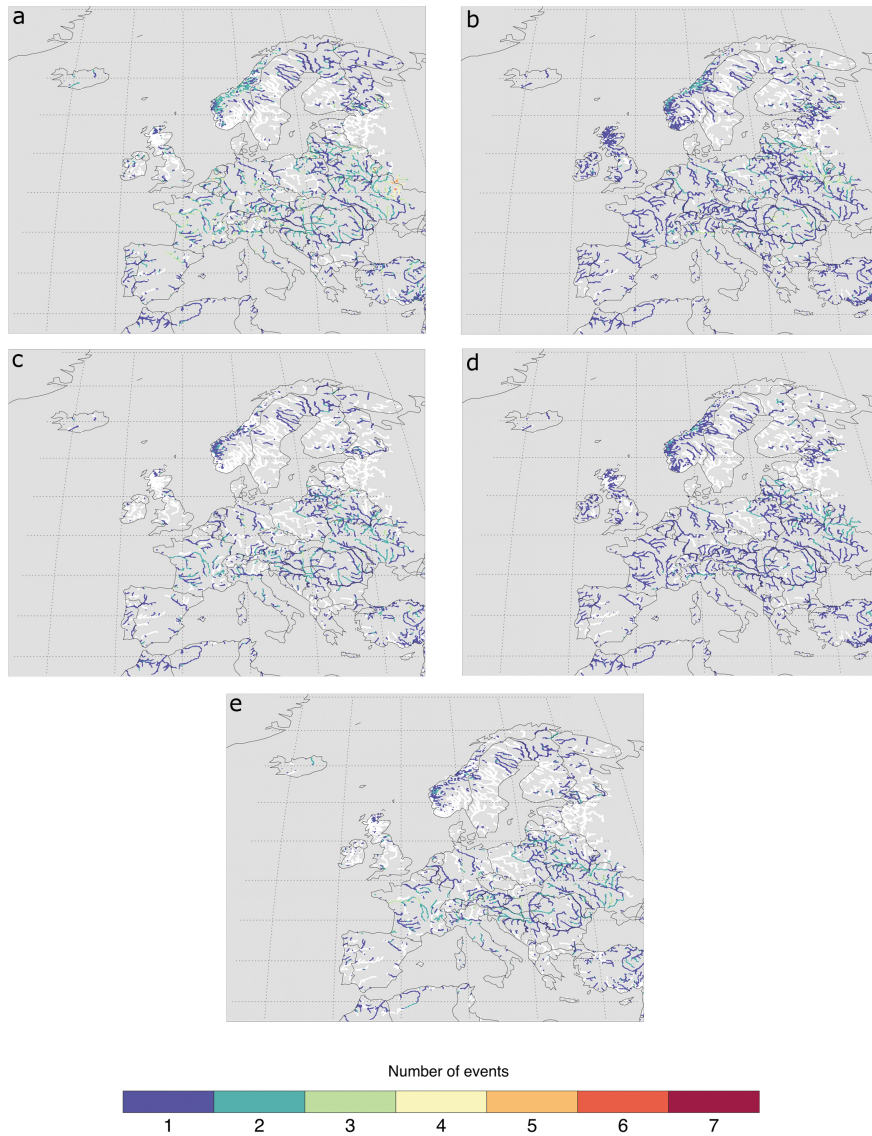


Figure B1. Forecasted drought occurrences (median of 25 ensemble members) in the European rivers using different drought identification methods and the forecast initiated on 1th July 2003 with a lead time 7-month for: a) the VTD, b) the FTD, c) the VTM, d) the FTM, and e) the SSI-1 approaches. White river color indicates that no drought was forecasted.

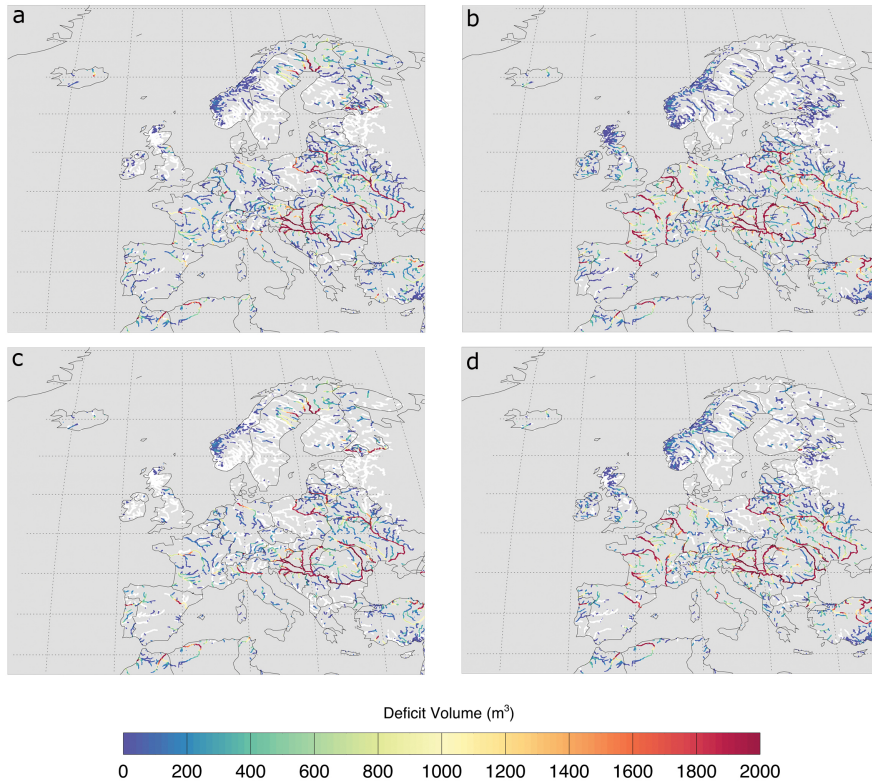


Figure B2. Forecasted average drought deficit volume (median of 25 ensemble members) in the European rivers using different drought identification methods and the forecast initiated on 1st July 2003 with a lead time 7-month for: a) the VTD, b) the FTD, c) the VTM, d) the FTM, and e) the SSI-1 approaches. White river color indicates that no drought was forecasted. Note that deficit volume is not standardized.